

Stereoselective Ring-Opening Polymerization of a Racemic Lactide by Using Achiral Salen- and Homosalen-Aluminum Complexes

Nobuyoshi Nomura,^{*[a]} Ryohei Ishii,^[a] Yoshihiko Yamamoto,^[b] and Tadao Kondo^[a]

Abstract: Highly isotactic polylactide or poly(lactic acid) is synthesized in a ring-opening polymerization (ROP) of racemic lactide with achiral salen- and homosalen-aluminum complexes (salenH₂ = *N,N'*-bis(salicylidene)ethylene-1,2-diamine; homosalenH₂ = *N,N'*-bis(salicylidene)trimethylene-1,3-diamine). A systematic exploration of ligands demonstrates the importance of the steric influence of the Schiff base moiety on the degree of isotacticity and the backbone for high activity. The complexes prepared in situ are pure enough to apply to the polymerizations without purification. The crystal structures of the key complexes are elucidated by X-ray diffraction, which confirms that they are chiral. However, analysis of the ¹H and ¹³C NMR spec-

tra unambiguously demonstrates that their conformations are so flexible that the chiral environment of the complexes cannot be maintained in solution at 25 °C and that the complexes are achiral under the polymerization conditions. The flexibility of the backbone in the propagation steps is also documented. Hence, the isotacticity of the polymer occurs due to a chain-end control mechanism. The highest reactivity in the present system is obtained with the homosalen ligand with 2,2-dimethyl substituents in the backbone (ArCH=NCH₂CMe₂CH₂N=CHAr),

Keywords: aluminum • homogeneous catalysis • lactides • polymers • ring-opening polymerization

whereas *t*BuMe₂Si substituents at the 3-positions of the salicylidene moieties lead to the highest selectivity ($P_{meso} = 0.9_8$; $T_m = 210^\circ\text{C}$). The ratio of the rate constants in the ROPs of racemic lactide and L-lactide is found to correlate with the stereoselectivity in the present system. The complex can be utilized in bulk polymerization, which is the most attractive in industry, although with some loss of stereoselectivity at high temperature, and the afforded polymer shows a higher melting temperature ($P_{meso} = 0.9_2$, T_m up to 189 °C) than that of homochiral poly(L-lactide) ($T_m = 162\text{--}180^\circ\text{C}$). The “livingness” of the bulk polymerization at 130 °C is maintained even at a high conversion (97–98 %) and for an extended polymerization time (1–2 h).

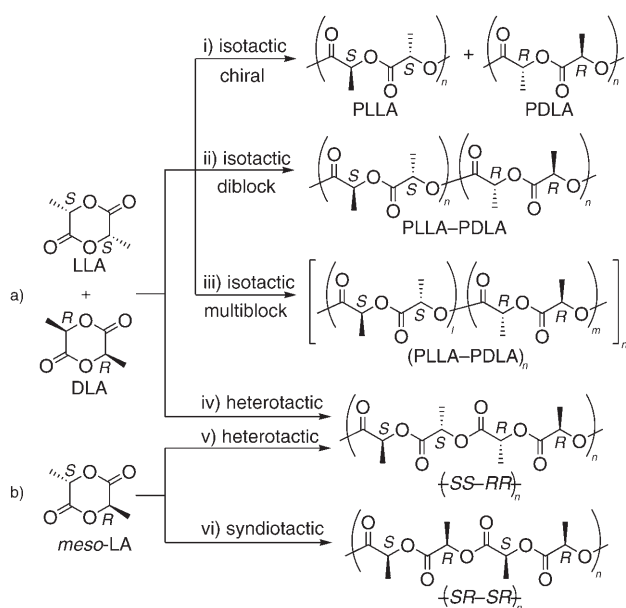
Introduction

Recent concerns about our environment have led to a search for environmentally benign and sustainable materials that could substitute the more commonly used petroleum-based materials. Biodegradable and sustainable polylactide (PLA) is becoming one of the most promising and practical materials as a partial replacement for petroleum-based materials.^[1] Commercially available PLA is generally homochiral poly(L-lactide) (PLLA) at present because L-lactic acid with high optical purity can be obtained in bulk by fermentation of carbohydrates. PLLA is mostly synthesized by the ring-opening polymerization (ROP) of homochiral L-lactide (LLA), which is a cyclic dimer of L-lactic acid. Due to the asymmetric methine carbon of lactic acid there are three possible stereoisomers of lactide, namely LLA, D-lactide (DLA), and *meso*-lactide (*meso*-LA; Scheme 1). The high purity of LLA is crucial for the desired physical and mechanical properties because contamination by DLA and/or

[a] Dr. N. Nomura, Dr. R. Ishii, Prof. Dr. T. Kondo
Laboratory of Polymer Chemistry
Graduate School of Bioagricultural Sciences
Nagoya University
Nagoya 464-8601 (Japan)
Fax: (+81) 52-789-4012
E-mail: nnomura@nagoya-u.jp.

[b] Dr. Y. Yamamoto
Department of Applied Chemistry
Graduate School of Science and Engineering
Tokyo Institute of Technology
Meguro, Tokyo 152-8552 (Japan)

Supporting Information for this article is available on the WWW under <http://www.chemeurj.org/> or from the author. Crystal structures of **8**, **9**, **10**, and **11**; ¹H, ¹³C, and ¹H-¹H COSY NMR of complexes **9** and **11**, and homonuclear decoupled ¹H NMR spectra of the methine regions of poly(*rac*-LA) prepared with Al(O*i*Pr)₃, **8**, and **9**; plots of time versus ln[*rac*-LA]₀/[*rac*-LA]_t and plots of ln[Al]₀ versus ln*k*_{(*rac*)app} in the polymerization of *rac*-LA with complex **9**.



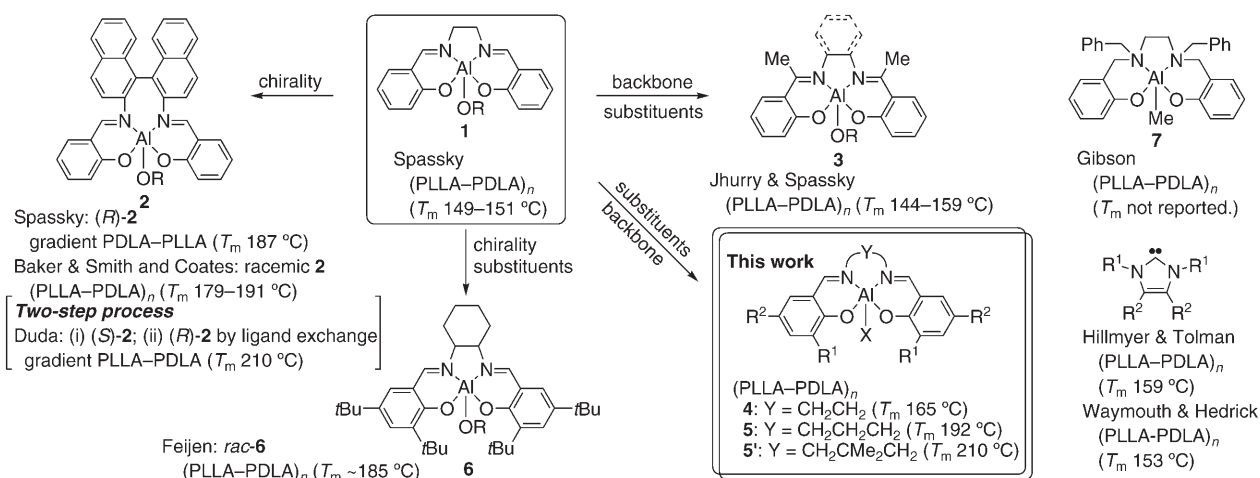
Scheme 1. Ultimate microstructure patterns of PLA obtained from *rac*-LA and *meso*-LA.

meso-LA makes the PLA amorphous due to stereoirregularity.^[2]

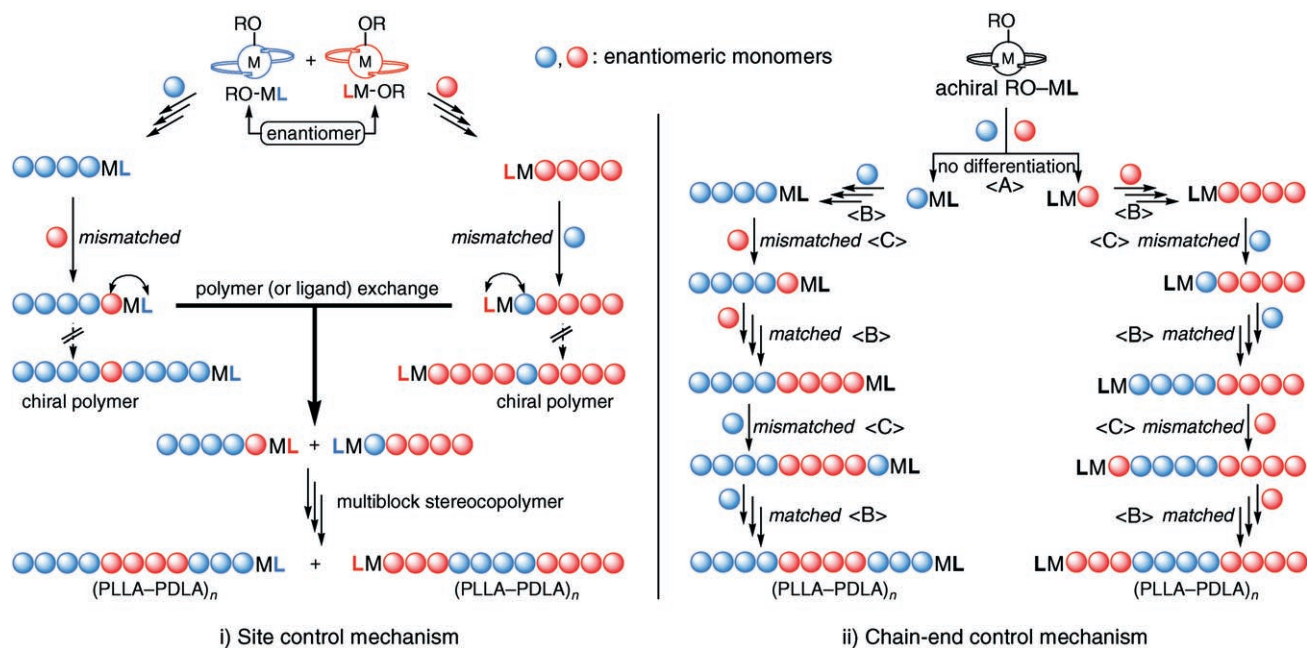
An interesting thermal property of PLA has been reported by Ikada and Tsuji—the melting temperature (T_m) is raised upon stereocomplex formation of PLLA with poly(D-lactide) (PDLA).^[3] Specifically, the T_m value of homochiral PLLA or PDLA is 162–180 °C,^[4] while that of the stereocomplex between PLLA and PDLA is 230 °C. Because PLA starts to decompose when heated above its T_m ,^[5] this stereocomplex formation is an attractive technique to improve its thermal stability. Stereocomplex formation of the diblock polymer PLLA-*b*-PDLA has also been reported ($T_m \approx 205$ °C).^[6]

It is known that the ROP of racemic lactide (*rac*-LA) using conventional catalysts such as $\text{Al}(\text{O}i\text{Pr})_3$ ^[7] and $\text{Sn}(\text{2-ethylhexanoate})_2$ ^[8] produces nearly atactic PLA, which is amorphous and less attractive as a material. Synthetic chemists have studied the stereoselective polymerization of *rac*-LA for the synthesis of the thermally more stable PLA in one step as well as for the synthetic challenge of controlling the stereoregularity.^[9] The ROP of *rac*-LA may produce two ultimate stereoregular patterns—*isotactic* and *heterotactic* polymers (Scheme 1a)—if the ring-opening reaction occurs via a coordination–insertion mechanism without racemization.^[10] The *isotactic* PLA obtained from *rac*-LA can be divided into three kinds of PLA: i) each polymer molecule is homochiral; ii) a diblock stereocopolymer,^[11,12a] and iii) a multiblock stereocopolymer.^[13–22] The alternate polyadditions of LLA and DLA produce heterotactic^[23] PLA (Scheme 1a(iv)). The ROP of *meso*-LA can also produce heterotactic^[17] and syndiotactic^[17,24] PLA (Scheme 1b). As shown in Scheme 1, PLAs with a variety of microstructures can be synthesized by the stereoselective ROP of *rac*-LA and *meso*-LA. Among these PLAs, the *isotactic* and *syndiotactic* ones are crystalline.

One of the first catalysts developed for the stereoselective polymerization of *rac*-LA into *isotactic* PLA was reported by Spassky, who used achiral salen^[25] ligand–Al complexes^[13a] (**1**, Scheme 2) to synthesize the multiblock stereocopolymer (PLLA–PDLA)_{*n*}^[13b] ($T_m = 149$ – 151 °C). A one-step synthesis of gradient PDLA–PLLA was also reported by Spassky using homochiral (*R*)-**2**,^[11] and this was the first synthetic success in obtaining PLA from *rac*-LA, which is thermally more stable than homochiral PLLA due to stereocomplex formation ($T_m = 187$ °C). Baker, Smith, and Coates have reported that the racemic complex **2** polymerizes *rac*-LA more efficiently^[15–17] ($T_m = 179$ – 191 °C) than homochiral (*R*)-**2**, although the microstructures of the PLAs obtained from (*R*)-**2** and racemic **2** were different.^[26] It was believed at first that each enantiomer of **2** preferably polymerizes one of the enantiomeric monomers



Scheme 2. Catalysts for the synthesis of isotactic poly(lactide) from racemic lactide in a one-step process.



Scheme 3. Isotactic polymer sequences via i) a site control mechanism (SCM) and ii) a chain-end control mechanism (CEM).

consistently to afford the chiral polymer molecules. However, Coates subsequently found that each polymer molecule was actually a multiblock stereocopolymer by precise microstructure analysis of the polymers.

Gibson, Jhurry, Spassky and their co-workers have examined the effects of the substituents on the salen ligand; they obtained a slightly enhanced stereoselectivity using complex **3**^[14,18] ($T_m = 144\text{--}159^\circ\text{C}$). We have focused on the effects of the backbone that connects the two Schiff bases and the substituent effects (R^1) of the salicylidene moieties (complexes **4** and **5**)^[19] (T_m up to 192°C with $R^1 = R^2 = t\text{Bu}$). This was the first report of the effect of introducing bulky substituents at the 3-position of the salicylidene moieties in the stereoselective polymerization of *rac*-LA.^[27] Feijen and co-workers subsequently utilized a racemic and homochiral bulky Jacobsen ligand–Al complex (**6**)^[20] to obtain a polymer with a T_m of around 185°C . Recently, Duda and Majerska reported a new approach for achieving extremely high stereoselectivity (T_m up to 210°C) using *chiral* complex **2**, where a two-step technique that involves homochiral ligand exchange at 50% of monomer conversion was applied in a one-pot reaction.^[12a] Surprisingly, the T_m value of this gradient diblock PLLA–PDLA polymer (210°C) is higher than that of the polymer obtained by step-by-step synthesis of PLLA-*b*-PDLA (205°C).^[6] Gibson and co-workers have also discovered dramatic substituent effects with the “salan” ligand and has achieved a moderate isotactic polymerization of *rac*-LA using **7**.^[21] Finally, some unique and intriguing organic catalysts have been developed by Hillmyer, Tolman, Waymouth, Hedrick and co-workers.^[22]

From a mechanistic point of view there are two ways to get stereoselectivity: by a site control mechanism^[28] (SCM) or a chain-end control mechanism (CEM). In the SCM

(Scheme 3(i)), the complex has a chiral environment that is constructed by the ligand around the metal center and can consistently differentiate LLA from DLA, preferentially reacting with one enantiomer. Although each polymer molecule obtained by an SCM is supposed to be optically active,^[29] Coates has shown that the polymer molecules have multiblock stereosequences because polymer exchange occurs during the polymerization when the mismatched monomer is incorporated.^[16] The poly(*rac*-LA) obtained by an SCM is thermally more stable than homochiral PLLA (polymers obtained with complexes **2** and **6**, respectively). In contrast, isotactic polymerization via a CEM has not yet proved possible, despite the pioneering work of Spassky and co-workers with the achiral salen complex **1**.^[13] In a polymerization that occurs by a CEM^[23a] both the metal complex and the ligand are achiral. The initiation reaction occurs without enantiomeric differentiation of the racemic monomer (<A>, Scheme 3(ii)), which means that the chirality is incorporated into the propagating chain end. The monomer with the same chiral sense as that of the inserted monomer is then preferentially incorporated into the propagating chain end (). Once a mismatched monomer has been incorporated (<C>), the monomer with the same chiral sense as that of the propagating chain end, in other words the mismatched monomer just before it, turns into a matched monomer in the next propagation step (). If ultimate stereoselectivity is achieved, each polymer is homochiral (Scheme 1a(i)), although the combination of polymer molecules is optically inactive. In reality, polymerization by a CEM affords a multiblock stereocopolymer (PLLA–PDLA)_n due to several inversions of the chiral sense of the incorporated monomer. The segmental exchange of the homochiral PLLA and PDLA chains by a few intermolecular

transesterifications also affords multiblock stereocopolymers, while they can be disregarded in the case of ideal living polymerization systems.

Herein, we report the details of our investigations into the stereoselective ROP of *rac*-LA using achiral Al complexes. The structures of some new Al complexes are elucidated by X-ray crystallography and ^1H and ^{13}C NMR spectroscopy, and a hypothetical model for isotacticity is proposed on the basis of our experimental results. We also show that the ratio of the rate constants (k_p 's) in the ROPs of *rac*-LA and LLA corresponds with the stereoselectivity in the present system. Furthermore, the Al complex is utilized in bulk polymerization at 130–180 °C, and the obtained PLAs show higher melting temperatures than that of homochiral PLLA. The livingness is maintained even at high monomer conversion (98 %) at 130 °C.

Results and Discussion

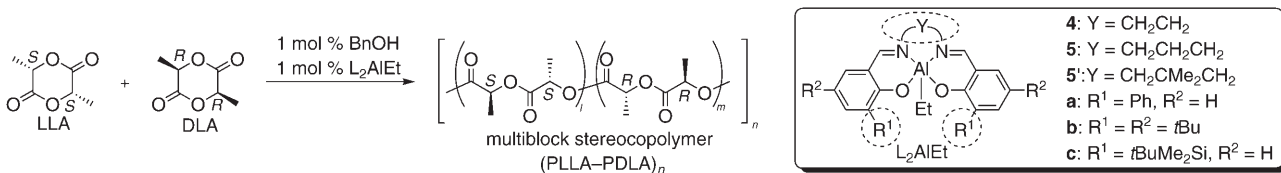
Ligand design: At the outset of our studies on the stereoselective ROP of *rac*-LA, we first examined various complexes prepared in situ to develop an efficient ligand system.^[30] The most promising complexes were then isolated in order to investigate the polymerization in greater detail. Two series of substituted complexes **4** and **5** (X = Et, Scheme 2), whose ligands are achiral and can be easily modified, were examined. Both of them were prepared simply by mixing AlEt_3 and each ligand at 70 °C in toluene.^[31] In the presence of 1 mol % of benzyl alcohol (BnOH), complexes **4** and **5** (1 mol %) polymerized *rac*-LA at 70 °C (Table 1). The crude reaction mixtures were analyzed to obtain the conversion of *rac*-LA, the number-average molecular weight (M_n), and polydispersity index (PDI) by ^1H NMR spectroscopy and size-exclusion chromatography (SEC). The ^1H and ^{13}C NMR spectra of the obtained poly(*rac*-LA)s indicated that they are isotactic multiblock stereocopolymers (PLLA-PDLA) $_n$.^[32] P_{meso} is the probability of a *meso*-linkage of the tetrad between lactide units, and we calculated this from the ^{13}C NMR spectrum.^[33] The T_m values, which correlated strongly with the tacticity of poly(*rac*-LA), were obtained by differential scanning calorimetry (DSC) after purification of the polymer by precipitating in cold MeOH. We first performed a series of experiments with the salen-Al complexes **4**. The polymerization with the complex with no substituents on the salen ligand ($\text{R}^1 = \text{R}^2 = \text{H}$) was slow, as reported previously by Spassky,^[34] and the conversion was 62 % after 26 h (Table 1, entry 1). Amongst the substituted complexes (Table 1, entries 2–5), the more sterically demanding ones raised the P_{meso} and T_m values the most (Table 1, entries 4 and 5). The Ph-substituted complex **4a** clearly shows both high reactivity and good selectivity (Table 1, entry 4), and the stereoselectivity of the bulky *t*Bu-substituted complex **4b** is as high as that of **4a**, although the polymerization is much slower (Table 1, entry 5).

The homosalen-Al complex **5**, which is a homolog of salen complex **4**, had not been examined in the polymeri-

zation of *rac*-LA before our preliminary studies.^[19a] The catalytic activities of the homosalen complexes **5** were found to be much higher than that of their analogues **4**.^[35] As the substituents become larger, P_{meso} and T_m generally increase and the polymerization rate decreases (Table 1, entries 6–9, 13, and 14). Ph-substituted **5a** is notable not only because it gives highly isotactic poly(*rac*-LA) but also because the polymerization rate is comparable to that of the simple homosalen complex (cf. Table 1, entries 6 and 9). It is likely that the Ph substituents in the salen and homosalen systems act as electronic tuning substituents^[36] that enhance the polymerization rate. Because the polymerization rate of **5a** is high, a smaller amount of **5a** (0.33 mol %) and BnOH (0.33 mol %) was used for the synthesis of poly(*rac*-LA) with a high M_n . The polymerization proceeded without any difficulties to afford isotactic poly(*rac*-LA) with an M_n approximately three times greater than that reported above (Table 1, entry 9) after 4.5 h and with a small PDI (Table 1, entry 10). The possibility of this immortal polymerization, in which the number of polymer molecules is controlled by the amount of alcohol, was also examined.^[37] *rac*-LA was polymerized in the presence of 0.33 mol % of **5a** and 1.0 mol % of BnOH (3 equiv. with respect to **5a**). After 2.8 h, poly(*rac*-LA) that was almost identical to that in entry 9 (1 mol % of **5a** and BnOH to *rac*-LA) was obtained (Table 1, entry 11). The polar solvent THF slows down the polymerization, as expected,^[38] while the resultant isotacticity was comparable to that in toluene (Table 1, entry 12). To obtain a higher stereoselectivity with a high catalytic activity, the two Ph groups of **5a** were replaced by bulkier 3,5-di-*tert*-butylphenyl (*t*Bu $_2$ C $_6$ H $_3$ -) groups. The isotacticity increased, as expected, but the polymerization rate decreased considerably (see entries 9 and 13 in Table 1).

The sterically demanding complex **5b** produced poly(*rac*-LA) with high P_{meso} and T_m values (0.9 $_2$ and 192 °C, respectively). In addition, bulky substituents such as Ph and *t*Bu appeared to be effective in keeping the PDIs low in toluene (see Table 1, entries 6–8, 9–11, 13, and 14). Introduction of Cl at the R 2 position^[14] decreased the catalytic activity to some extent (Table 1, entry 15), which suggests that the balance of Lewis acidity of the Al center should be important for controlling the polymerization rate. Me $_3$ Si groups at the R 1 position hindered the polymerization of *rac*-LA (Table 1, entry 16) compared with *t*Bu groups (Table 1, entry 14), whereas a Ph group at R 2 showed ambiguous effects on the polymerization rate (Table 1, entry 17). The complex **5** with R $^1 = \text{R}^2 = \text{Br}$ gave a result comparable to that with the simple homosalen-Al complex except for their polydispersities (see Table 1, entries 6 and 18).

We then modified the backbone of complex **5**^[39,40] as the backbone connecting the two Schiff bases significantly influences the catalytic activity of the complexes. The polymerization rate of the dimethyl-substituted complex **5a** is clearly higher, and the conversion of *rac*-LA reached 93 % after 0.4 h with good stereoselectivity (see Table 1, entries 9 and 19). The high reactivity of **5a** appeared to be an attractive feature for the “catalytic” synthesis of a number of poly(*rac*-

Table 1. Screening of salen and homosalen ligands.^[a]


Entry	Y	R ¹	R ²	Time [h]	Conv. ^[b] [%]	M _n ^[c] × 10 ⁻³	PDI ^[c]	P _{meso} ^[d]	T _m ^[e] [°C]
1	CH ₂ CH ₂	H	H	26	62	8.0	1.2 ₆	0.7 ₂	— ^[f]
2		Me	Me	40	72	10.2	1.2 ₄	0.6 ₉	— ^[f]
3		<i>i</i> Pr	<i>i</i> Pr	40	32	4.7	1.0 ₈	0.7 ₈	153
4		Ph	H	5.2	79	14.1	1.2 ₃	0.8 ₂	165
5		<i>t</i> Bu	<i>t</i> Bu	72	19	5.3	1.0 ₇	0.7 ₉	163
6	CH ₂ CH ₂ CH ₂	H	H	1.3	93	20.8	1.2 ₉	0.7 ₇	(146)
7		Me	Me	1.8	95	23.0	1.3 ₆	0.7 ₈	(147)
8		<i>i</i> Pr	<i>i</i> Pr	3	95	18.3	1.2 ₉	0.8 ₂	(161)
9		Ph	H	1.3	94	20.0	1.1 ₁	0.8 ₃	170
10 ^[g]		Ph	H	4.5	93	59.5	1.0 ₇	0.8 ₂	170
11 ^[h]		Ph	H	2.8	93	21.8	1.0 ₈	0.8 ₂	167
12 ^[i]		Ph	H	18	93	19.4	1.2 ₄	0.8 ₃	169
13		<i>t</i> Bu ₂ C ₆ H ₃ ^[j]	Me	7	91	21.9	1.0 ₅	0.8 ₆	185
14		<i>t</i> Bu	<i>t</i> Bu	14	95	22.4	1.0 ₆	0.9 ₂	192
15		<i>t</i> Bu	Cl	22	95	20.1	1.0 ₆	0.9 ₀	192
16		Me ₃ Si	H	24	80	16.1	1.0 ₆	0.9 ₀	192
17		Me ₃ Si	Ph	12	75	12.5	1.0 ₆	0.9 ₂	192
18		Br	Br	1.3	86	22.8	1.0 ₇	0.7 ₆	(142)
19	CH ₂ CMe ₂ CH ₂	Ph	H	0.4	95	20.2	1.0 ₅	0.8 ₅	171
20 ^[h]		Ph	H	2	90	22.7	1.0 ₉	0.8 ₅	171
21 ^[k]		Ph	H	8	91	23.1	1.0 ₈	0.8 ₄	171
22		<i>t</i> Bu	<i>t</i> Bu	6	93	20.2	1.0 ₆	0.9 ₃	192
23		Me ₃ Si	H	5	90	19.3	1.0 ₆	0.9 ₂	192
24		Me ₃ Si	Ph	4	93	19.9	1.0 ₅	0.9 ₂	193
25		Et ₃ Si	H	12	93	20.5	1.0 ₈	0.9 ₅	199
26		Et ₃ Si	CF ₃	8	66	13.3	1.0 ₈	0.9 ₅	201
27 ^[l]		<i>t</i> BuMe ₂ Si	H	19	62	10.3	1.1 ₃	0.9 ₇	207
28				19	93	20.0	1.0 ₉	0.9 ₇	207
29		Ph ₃ Si		19	0	—	—	—	—
30		<i>i</i> Pr ₃ Si		19	0	—	—	—	—
31		<i>t</i> BuPh ₂ Si		19	0	—	—	—	—
32		(<i>n</i> Bu) ₃ Sn		30	90	14.9	1.0 ₈	0.8 ₈	183
33 ^[m]	CH ₂ CEt ₂ CH ₂	<i>t</i> Bu	<i>t</i> Bu	6	38	6.9	1.0 ₇	0.9 ₂	189
34 ^[m]	CH ₂ CBn ₂ CH ₂	<i>t</i> Bu	<i>t</i> Bu	6	57	14.3	1.0 ₆	0.8 ₈	175
35	CH ₂ SiMe ₂ CH ₂	Me ₃ Si	Ph	54	90	18.5	1.0 ₆	0.8 ₈	177

[a] Unless otherwise noted, the polymerizations were performed under N₂ in toluene with the following conditions: [rac-LA]/[Al] = 100/1. Each catalyst was prepared in situ by mixing each ligand and Et₃Al at room temp. for 1 h (entries 1–4), at room temp. for 3 h (entry 5), at 70 °C for 1 h (entries 6–13), at 70 °C for 3 h (entries 14–18, 27, and 33–34), at 70 °C for 6 h (entries 19–22), or at 70 °C for 12 h (entries 23–26, 28–32, and 35). The mixture of each catalyst was transferred into the mixture of rac-LA and BnOH through a cannula. [b] Determined by ¹H NMR spectroscopy (300 MHz). [c] M_n: number-average molecular weight. PDI: polydispersity index (M_w/M_n). Both were obtained for the crude reaction mixtures by SEC (CHCl₃, polystyrene standards). The M_n values in this paper are consistently estimated by SEC and are typically higher than the expected ones due to the hydrodynamic volume difference between PLA and polystyrene.^[41] [d] P_{meso} is the probability of a meso linkage between lactide units and was calculated from the ¹³C NMR spectra of the obtained poly(rac-LA): [mmm] = P_{meso}(P_{meso}+1)/2; [mmr] = P_{meso}(1-P_{meso})/2; [rmm] = P_{meso}(1-P_{meso})/2; [rmr] = (1-P_{meso})²/2; [rrm] = (1-P_{meso})/2. [e] Measured by DSC after precipitation with cold MeOH. T_m values were recorded in the second run. The data in parentheses were obtained in the first run because the T_m could not be detected in the second run due to slow crystallization. [f] Not detected. [g] L₂AlEt (0.33 mol %) and BnOH (0.33 mol %) were used. [h] L₂AlEt (0.33 mol %) and BnOH (1.0 mol %) were used. [i] THF was used as the solvent. [j] 3,5-Di-*tert*-butylphenyl. [k] L₂AlEt (0.10 mol %) and BnOH (1.0 mol %) were used. [l] The complex was prepared at 70 °C for 3 h. [m] Data taken from reference [39b].

LA) molecules. Using one-third of the amount of **5a** (0.33 mol %) relative to BnOH (1.0 mol %; Table 1, entry 20) or one-tenth of the amount of **5a** (0.10 mol %) relative to BnOH (1.0 mol %; Table 1, entry 21) produced virtually the same poly(rac-LA) as the “stoichiometric” reaction of entry 19 (1.0 mol % **5a** and 1.0 mol % BnOH); in

both cases the P_{meso} and T_m values were essentially identical. Complex **5b** also polymerized rac-LA faster than **5b** (see Table 1, entries 14 and 22). Bulkier silyl groups, which are easily modified, were then introduced into the ligands (Table 1, entries 23–31). The highest selectivity was obtained with *t*BuMe₂Si-substituted **5c** (Table 1, entries 27 and 28).

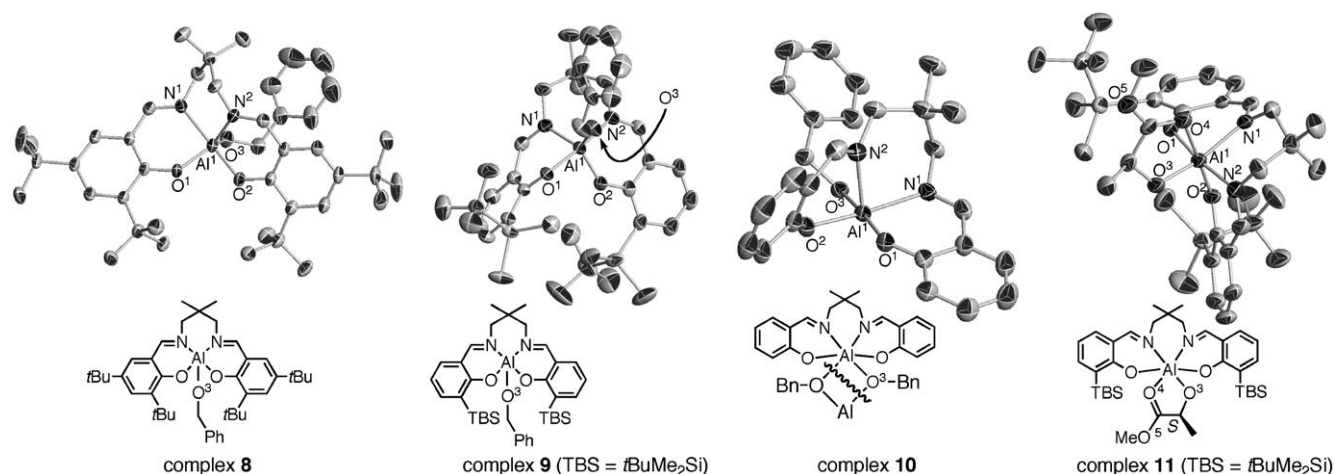


Figure 1. Crystal structures of homosalen–Al complexes. Hydrogen atoms have been omitted for clarity.

Complex **5c**, which was prepared at 70 °C for 3 h, produced poly(*rac*-LA) with a rather low M_n (expected M_n of about 13000 by SEC at 62% conversion; Table 1, entry 27). Direct analysis of the crude polymerization mixture by SEC gave a bimodal trace, one of which had a strong UV absorption. However, after washing the crude polymer in toluene with 1 N aqueous HCl the UV absorption disappeared and the SEC trace of the polymer became monomodal with a small PDI value. These experiments made us suspect that some of the ligand that is not bound to the aluminum center might have served as an initiation terminus because of the short preparation time of the complex. In fact, **5c** prepared at 70 °C for 12 h produced poly(*rac*-LA) with the expected M_n in a shorter time (Table 1, entry 28). The data in entries 27 and 28 indicate that the stereoselectivity is not influenced by percentage of complex formed in situ whereas the rate of polymerization and the M_n value are.

The complexes with more sterically demanding substituents failed to polymerize *rac*-LA at all (Table 1, entries 29–31). An (*n*Bu)₃Sn group at the R¹ position slowed down the polymerization (Table 1, entry 32), and bulkier substituents in the backbone decreased the isotacticity of the poly(*rac*-LA)s (Table 1, entries 33 and 34). The longer bonds of the backbone containing two Si–C bonds decreased the stereoselectivity (see Table 1, entries 24 and 35). An extensive screening of the ligands therefore allowed us to find a system for an efficient stereoselective ROP of *rac*-LA that gives isotactic poly(*rac*-LA). As shown in Table 1, crystalline poly(*rac*-LA)s with various T_m values (153–207 °C) can be synthesized without changing the composition simply by varying the ligands, which may make this a useful method to design temperature-sensitive materials.

Structures of homosalen–Al complexes and the origin of stereoselectivity

Structure determination by X-ray diffraction: The highly stereoselective homosalen–Al alkoxide complexes **8**^[42] and **9**^[43] were isolated (Figure 1) on the basis of the experiments

using various complexes prepared in situ. Their X-ray structures showed that they are monomeric pentacoordinate complexes that are chiral in the solid state. The τ value of a complex indicates how closely a distorted pentacoordinate complex approximates either a trigonal-bipyramidal (tbp, $\tau=1$) or a square-pyramidal (sqp, $\tau=0$) geometry.^[44] The two largest angles in each complex are 171.55° ($\angle O^1\text{--Al}^1\text{--N}^2$) and 122.67° ($\angle O^2\text{--Al}^1\text{--N}^1$) in complex **8** and 171.95° ($\angle O^1\text{--Al}^1\text{--N}^2$) and 122.08° ($\angle O^3\text{--Al}^1\text{--O}^1$) in complex **9**. The τ values^[27] of **8** and **9** are 0.815 and 0.831, respectively, which means that their geometries in the solid state tend towards tbp rather than sqp. The τ value of an Al(O*i*Pr) complex of **8** (AlOBn), which was isolated from the reaction between Al(O*i*Pr)₃ and the corresponding ligand under harsh conditions (toluene, 100 °C, 24 h), has been reported.^[40b] The large difference in the τ values between the AlOBn complex ($\tau=0.815$) and the Al(O*i*Pr) complex ($\tau=0.78$) indicates that the geometry of the complex is amenable to the alkoxide. In fact, the Al–O³ bond lengths in those complexes are more different (1.744 and 1.719 Å) than the other bonds (Table 2).

Table 2. Selected bond lengths [Å] around the Al center.

Bond	8	9	10	11
Al ¹ –O ¹	1.822 (1.818) ^[a]	1.823	1.841	1.842
Al ¹ –O ²	1.781 (1.774) ^[a]	1.788	1.839	1.829
Al ¹ –O ³	1.744 (1.719) ^[a]	1.736	1.908	1.840
Al ¹ –N ¹	1.992	1.980	2.062	2.048
Al ¹ –N ²	2.036	2.050	2.056	2.037
Al ¹ –O ⁴ (carbonyl)	–	–	–	2.165

[a] Data in parentheses are those of the Al–O*i*Pr complex; see reference [40b].

Complex **9**, which contains larger TBS substituents, has a higher τ value and approximates a tbp geometry more than complex **8**. The geometry of the monomeric salen–Al complex **4** (R¹=R²=*t*Bu, X=OEt; Scheme 2), whose τ value is 0.45^[45] and which shows a moderate stereoselectivity in the

ROP of *rac*-LA ($P_{meso}=0.7_9$; entry 5 in Table 1), is rather sqp. Considering these τ values, the *tbp* geometry of *salen*- and *homosalen*-Al complexes might be the key to the highly isotactic polymerization of *rac*-LA because the chirality of the polymer terminus bonding to the Al center can be amplified by the *tbp* geometry to construct a conformational chirality of the complex that will be much more effective for chiral recognition of the monomer. In contrast, the ultimate sqp geometry is achiral such that the chirality is localized only on the polymer terminus at the Al center.

The solubility of complex **10**^[46] is low in toluene. In an attempt to overcome this difficulty to obtain crystals for X-ray diffraction, γ -butyrolactone (BL) was added as a polar and relatively unreactive compound in the homopolymerization.^[47] Fortunately, X-ray quality crystals could be obtained from a BL/toluene solution. Although we expected that crystals of **10** with coordinated BL might be obtained,^[48] X-ray analysis showed a heterochiral (*meso* or Δ, Δ) dimeric structure without coordination of BL to **10**. The Al^I and O³ atoms in **10** are coordinated to the O^{3'} and Al^{I'} atoms of another complex, respectively.^[49] Half of the structure of dimeric **10**, the other half of which is crystallographically identical, is shown in Figure 1.

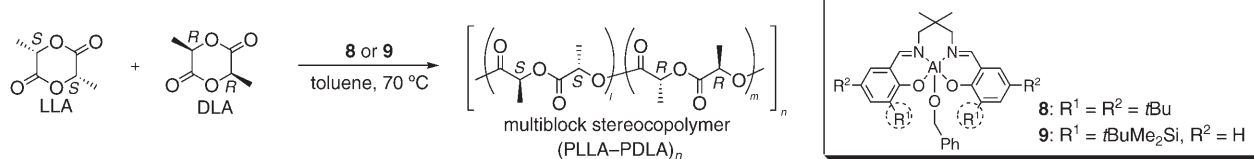
The reaction of **5'** ($R^1 = tBuMe_2Si$, $R^2 = H$, $X = Et$; Scheme 2) with methyl (*S*)-lactate afforded the hexacoordinate complex **11**.^[50] Coordination of the carbonyl oxygen of the lactate (O⁴) in the sixth position at the Al center has been proposed to occur in the stereoselective polymerization of *rac*-LA;^[12,17,51] this is therefore the first solid evidence of a complex with a *salen*-derived ligand in the stereoselective ROP of *rac*-LA as far as we know. Interestingly, Chen et al. have reached a different conclusion to us using an analogue of complex **8**: they concluded that the Al center does not coordinate to the oxygen atom of the acyl group in the ground state.^[12b]

The polymerization of *rac*-LA was re-examined with isolated complexes **8** and **9** (Table 3). The polymerization of *rac*-LA with **8** afforded isotactic poly(*rac*-LA) with M_n , PDI,

P_{meso} , and T_m values almost identical to those using **8** prepared in situ. This result supports the effectiveness of our initial strategy, that is, investigating the appropriate ligands by preparation of the Al complexes in situ. However, the isolated complex promotes the polymerization slightly faster. The formation of AlOR by the reaction of AlEt with HOR was found to be rather slow^[52] and could be monitored by ¹H NMR spectroscopy. Thus, the early stage of the polymerization by **8** prepared in situ is catalyzed by a small number of AlOR molecules with a fast chain-transfer with HOR. The M_n of the polymer is controlled by the molar ratio of *rac*-LA and the isolated complex (Table 3, entry 2). The stereoselectivity ($P_{meso}=0.9_8$, $T_m=208$ – 210 °C) is the highest in a one-step process with either achiral ($P_{meso}=0.88$ – 0.90 ,^[53] $T_m=193$ – 197 °C) or chiral complexes ($\alpha=0.98$ ^[17]), although a similar T_m value has been reported by Duda and Majerska in a two-step process using two chiral ligands.^[12a] The α value is larger than that of P_{meso} in the analysis of the same polymer microstructure because of its definition.^[17] The polymerization of *rac*-LA using 1.0 mol% of **9** in the presence of 1.0 mol% of BnOH (Table 3, entry 3) afforded a polymer similar to that in entry 2. Isolated **9** gave a poly(*rac*-LA) almost identical to that in entry 28 of Table 1, although the P_{meso} and T_m values were somewhat higher (Table 3, entry 4). The poly(*rac*-LA) with a higher M_n has a lower T_m . It has been reported previously that poly(*rac*-LA)s with higher M_n values have lower T_m values even with the same stereoselectivity.^[53]

Structure determination in solution by NMR spectroscopy: How rigid or flexible the geometry of the complex is in solution can be clarified by NMR studies. If complex **9** is chiral in solution as it is in the crystal structure, each of the two imine protons (ArCH=N) and four protons of the two methylenes (NCH₂CMe₂CH₂N) should be inequivalent. The flexible conformation of complex **8** has been investigated by us by ¹H and ¹³C NMR spectroscopy,^[54] although the much larger *t*BuMe₂Si groups of **9** might disturb the conformation-

Table 3. Polymerization of *rac*-LA using isolated complexes **8** and **9**.^[a]



Entry	Complex	<i>rac</i> -LA/Al/BnOH ^[b]	Time [h]	Conv. ^[c] [%]	M_n ^[d] $\times 10^{-3}$	PDI ^[d]	Yield ^[e] [%]	P_{meso} ^[f]	T_m ^[g] [°C]
1	8	100/1/0	5	94	21.2	1.0 ₈	90	0.9 ₂	192
2	9	50/1/0	6	88	11.1	1.0 ₉	82	0.9 ₈	210
3		100/1/1	12	93	10.7	1.1 ₃	92	0.9 ₇	208
4		100/1/0	14	96	22.0	1.0 ₇	91	0.9 ₈	209
5		200/1/0	24	95	43.9	1.0 ₉	94	0.9 ₈	205

[a] The polymerization conditions were identical to those in Table 1. [b] The initial mol ratio of *rac*-LA, the Al complex, and BnOH. [c] The conversion of *rac*-LA was measured by ¹H NMR spectroscopy. [d] M_n : number-average molecular weight (SEC) of the crude mixture; PDI: polydispersity index (M_w/M_n) of the crude mixture. [e] Precipitated with cold MeOH. [f] P_{meso} : the probability of a *meso* linkage between the lactide units. [g] Measured by DSC (T_m value in the second run).

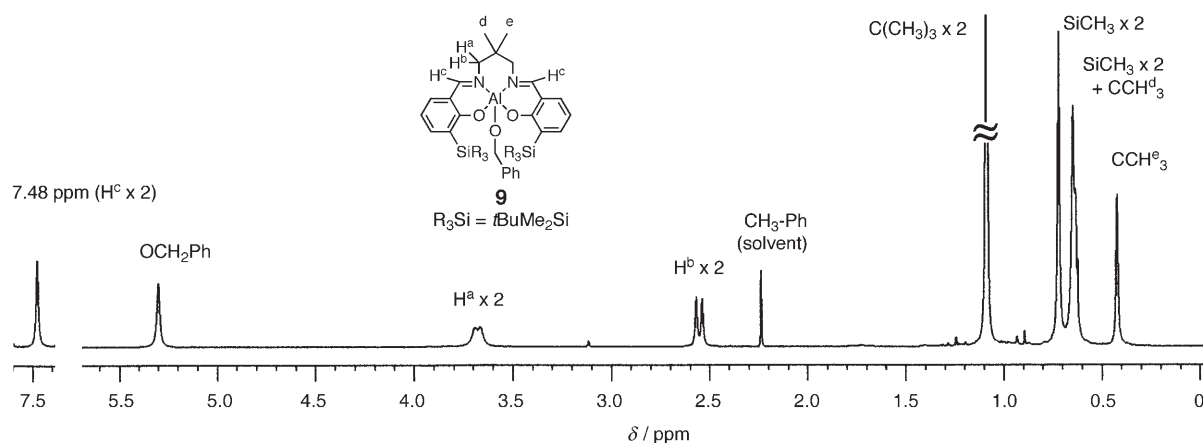
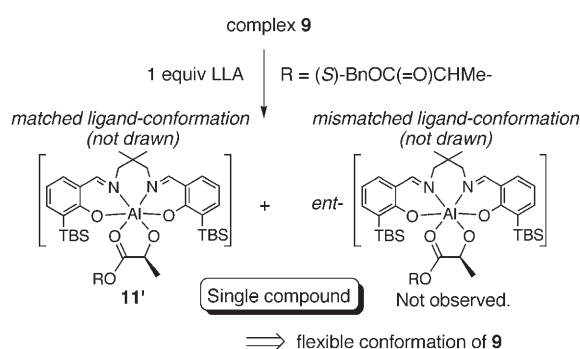
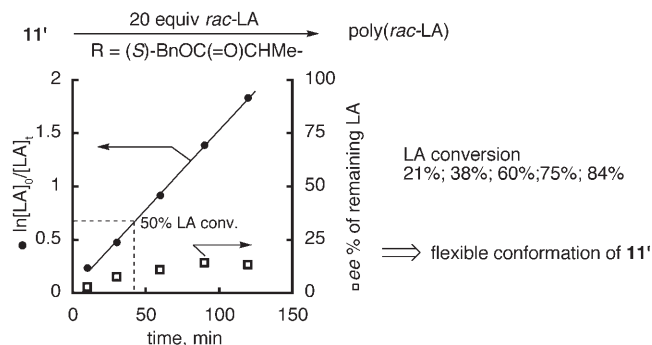


Figure 2. Aliphatic and imine regions of the ^1H NMR spectrum (400 MHz) of complex **9** in C_6D_6 .

a) Rigidity of the backbone in the initiation step.



b) Flexibility of the backbone in the propagation step.



Scheme 4. Polymerization of *rac*-LA using a homochiral complex.

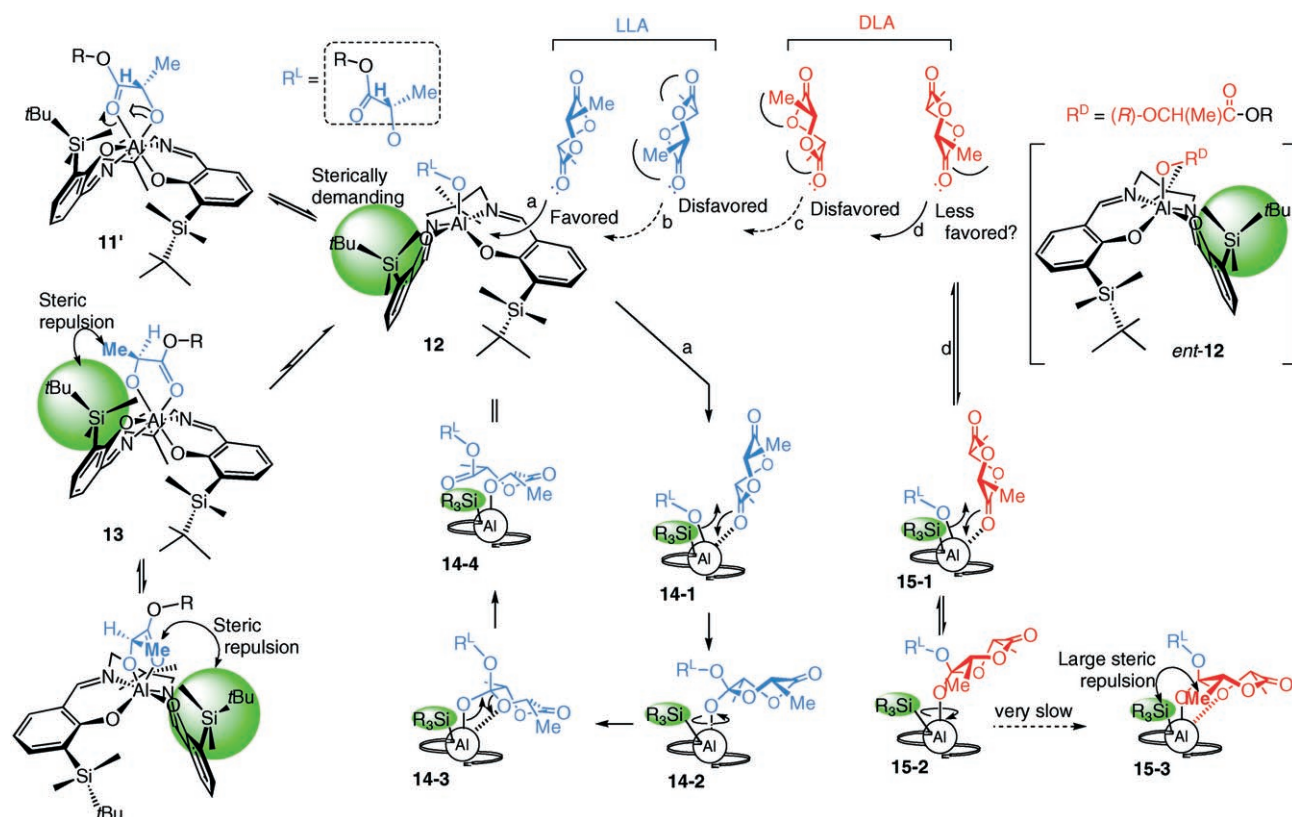
al flip of the geometry. The two protons of the imines ($2 \times \text{H}^c$) are equivalent in the ^1H NMR spectrum (Figure 2), and the diastereotopic protons of two methylenes ($2 \times \text{H}^a$ and $2 \times \text{H}^b$) appear at $\delta = 3.68$ (brd, $J = 10.8$ Hz; 2H) and 2.55 ppm (d , $J = 12.4$ Hz; 2H) with a geminal coupling; these correlations were confirmed by ^1H - ^1H COSY. The two diastereotopic CH_3 groups on the same Si atom appear at $\delta = 0.72$ (s, 6H; $2 \times \text{SiCH}_3$) and 0.65 ppm (s, 6H; $2 \times \text{SiCH}_3$). Since the dimethyl substituents in the backbone give two singlet peaks at $\delta = 0.64$ and 0.42 ppm in the ^1H NMR spectrum, the rigid chiral C_2 -symmetry of **9** in solution can also be excluded. The ^{13}C NMR spectrum (C_6D_6 , 100 MHz) shows only one imine carbon atom at $\delta = 168.70$ ppm and one methylene carbon of the backbone at $\delta = 34.98$ ppm. These NMR data indicate that the geometry of **9** is flexible in solution at 27°C on the NMR timescale, which is recognized “achiral”.

The dimeric complex **10** is nearly insoluble in benzene, therefore to obtain reasonable solubility we added between two equivalents and a large excess of BL relative to **10** due to our success in obtaining crystals for X-ray studies. However, we found that the precipitate and crystals of complex **10** were almost insoluble once formed, therefore further NMR analysis, except for the ^1H NMR spectrum of the major dimer, was not attempted.

The ^1H NMR spectrum of homochiral complex **11** shows characteristic changes from that of achiral complex **9**. For instance, two *t*Bu groups on the Si atom ($\delta = 1.12$ and 1.08 ppm) and the two imine protons ($\delta = 7.62$ and 7.54 ppm) appear as individual peaks. In addition, the two H^a protons in the backbone are shifted significantly to lower field ($\delta = 4.45$ ppm), while the H^b protons remain at almost the same chemical shift ($\delta = 2.63$ ppm; d , $J = 11.6$ Hz). The two imine carbons are inequivalent ($\delta = 167.55$ and 167.16 ppm), as are the methylene carbons of the backbone ($\delta = 71.56$ and 71.22 ppm). The carbonyl carbon of **11** appears at $\delta = 189.2$ ppm in the ^{13}C NMR spectrum. Its large downfield shift relative to the carbonyl carbon of free methyl lactate ($\delta = 176.1$ ppm) suggests that the oxygen atom of the carbonyl group should be coordinated by the Al atom of complex **11** in solution.^[55]

The mechanism of stereoselectivity: High stereoselectivity can be attributed to either an SCM or a CEM. Complex **9** has a chiral distorted trigonal-bipyramidal geometry in the crystal structure, while NMR studies show that its conformation is flexible in solution at ambient temperature.

The reaction of **9** and one equivalent of LLA at ambient temperature quantitatively affords complex **11'**, as shown in Scheme 4a. Its NMR data show the formation of a single



Scheme 5. A hypothetical model of the stereoselective ROP of *rac*-LA using **9**.

compound. If the geometry of **9** maintains a rigid chiral environment, two diastereomers should form. In this experiment, the geometry of the ligand should be flexible enough to be controlled by the chiral sense of the alkoxide. Regardless of the stable geometry of **9**, it is achiral in solution at ambient temperature due to its flexibility. Chiral differentiation of LLA and DLA by **9** might occur if the equilibrium of the chiral conformation is much slower than the initiation reaction. However, we decided to study the propagation step instead as this is where the stereodifferentiation mostly takes place.

An interesting stereocontrol situation may be occurring in the propagation step according to the literature.^[56] After the first monomer inserts into the Al–OBn bond of achiral complex **9**, a chirality derived from the monomer is introduced into the complex. In this process, the metal center and/or the ligand conformation may construct the strictly rigid chiral environment, which cannot be inverted by the exchange of the chiral sense of the polymer terminus. In this case, the stereoselective ROP of *rac*-LA proceeds via an SCM. The ROP of *rac*-LA was also examined with the homochiral complex **11'** (Scheme 4b). If the chiral environment around the metal center is rigid, the polymerization rate constant should be drastically diminished once the favored monomer LLA has been almost consumed at around 50% monomer conversion.^[11] However, the rate constant before and after 50% monomer conversion did not change until 84% monomer conversion. The enantiomeric excess of

the remaining monomer reaches a peak of around 13%, which indicates that the propagation reaction of both LLA and DLA take place simultaneously in this system. If the polymerization proceeds via an SCM, the enantiomeric excess should increase with monomer conversion, as reported by Spassky.^[11] These results prove that the chiral environment of the metal complex is flexible and that the chiral geometry of the complex can be inverted by introduction of the opposite chiral sense of the polymer terminus during the propagation reactions.

Because the origin of the chiral differentiation of the racemic monomers comes from the chiral sense of the last inserted monomer, we can conclude that the stereoselective polymerization of *rac*-LA using **9** takes place via a CEM. The chirality of the polymer terminus probably induces the chiral geometry of the flexible ligand, which amplifies the efficiency of the stereodifferentiation of LLA and DLA.

Even when the mechanistic details of asymmetric inductions remain unknown, hypothetical models that provide reasonable explanations for the stereoselectivity are useful for the design of other ligands/catalysts. However, such models are rare in the stereoselective ROP of *rac*-LA.^[57] A working model of the CEM with **9** is illustrated in Scheme 5 based on our extensive studies of substituent effects at the 3-position of the salicylidene moieties and the crystal structures of **9** and **11**. The most stable geometry of the Al alkoxide of alkyl (*S*)-lactate can be expected to be that of complex **11'**, according to the crystal structure of **11**. The decoor-

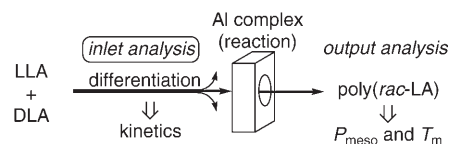
dination of the carbonyl oxygen from the Al center reorganizes the Al geometry to be pentacoordinate, as in complex **9**, which results in the formation of complex **12** and the opening-up of a coordination site for an approaching monomer. Rotation around the Al–OR^L bond (OR^L=(*S*)-OCH(Me)CO₂R) is disfavored due to the large steric repulsion between the TBS group and the methyl group of the lactate (complex **13**). The flipped geometry of the complex, as shown in complex **13'**, does not relieve the steric repulsion because the methyl group is still facing the other TBS group that covers the whole face of the lactate moiety. It is therefore apparent that complex **11'** is more stable than **13** and **13'**. Consequently, we assume that R in complex **11'** (or R^L in **12**) occupies the space behind one TBS group and that the monomer approaches the Al center only from the opposite open space (paths a–d) when the Al center is bonded to the alkoxide of alkyl (*S*)-lactate. It is clear that the geometry of **11** is not fixed in solution like that in the crystal structure due to detection of an NOE between the Me group of lactate ($\delta=1.63$ ppm) and the two *t*Bu moieties of the TBS groups ($\delta=1.12$ and 1.08 ppm) in the ¹H–¹H NOESY spectrum. However, the approach of *rac*-LA from the open side of **12** is most likely to be that illustrated in Scheme 5.

The LLA molecule, which keeps its methyl groups away from TBS, preferentially approaches the Al center from the open side opposite the R^L group in complex **12** to minimize the steric repulsion between its methyl groups and the TBS group and/or the R^LO group^[57] to afford complex **14-1** (path a \gg path b in Scheme 5). The alkoxide R^LO then attacks the carbonyl carbon to give complex **14-2**. After rotation around the Al–O bond to form the four-membered ring in **14-3**,^[17,58] the ring-opening reaction of LLA occurs to afford complex **14-4**. The geometry of the inserted LLA is arranged into the most favored conformation, with the polymer terminus of the alkoxide of alkyl (*S*)-lactate as in complexes **12** and **11'**, and the incorporation of LLAs occurs continuously. The approach of path a can be disturbed by bulkier substituent groups than TBS groups, as observed in entries 29–31 of Table 1.

Two approaches of DLA can also be imagined, although path c is unlikely for the same reasons as for path b.^[57] Path d, in which methyl groups are kept away from TBS, may take place, although some steric repulsion between the methyl group and the TBS group is expected (complex **15-1**). The alkoxide R^LO attacks the carbonyl carbon to give complex **15-2**. Although the ring-opening reaction of DLA requires the formation of the four-membered ring in **15-3** after the rotation around the Al–O bond,^[48] the large steric repulsion between the *t*BuMe₂Si group and the methyl group of DLA retards this step, and the reverse reaction into **15-1** and then decoordination of DLA into **12** occurs. However, once DLA has been incorporated into the polymer terminus somehow via path d (and/or possibly path c), the chirality of the polymer terminal OR^D (OR^D=(*R*)-OCH(Me)CO₂R) converts the geometry of the complex into *ent*-**12** as the most favorable geometry. DLA monomers are

then incorporated continuously into the polymer terminus until a disfavored LLA is incorporated.

Evaluation of the stereoselectivity from the kinetics of *rac*-LA and LLA polymerizations: The P_{meso} value obtained from the NMR analysis of poly(*rac*-LA) is a conventional evaluation of stereoselectivity, as is the evaluation from the T_m value. From the perspective of the reaction, both of them are analyses of the reaction product (output; Scheme 6). It occurred to us that the differentiation of the



Scheme 6. Analyses of stereoselectivity.

enantiomers of LLA and DLA by a CEM with **11** should be directly observable in their kinetics and that this would be another option to evaluate the stereoselectivity of catalysis at the *inlet* of the reaction. Such an approach in the stereoselective polymerization of *rac*-LA has not been achieved before.^[59] The ROP of *rac*-LA using complex **9**, which gave the highest isotacticity of poly(*rac*-LA), was carefully studied. Various parameters of the living ROP of *rac*-LA and LLA, and their relationships, are defined as shown in Scheme 7.

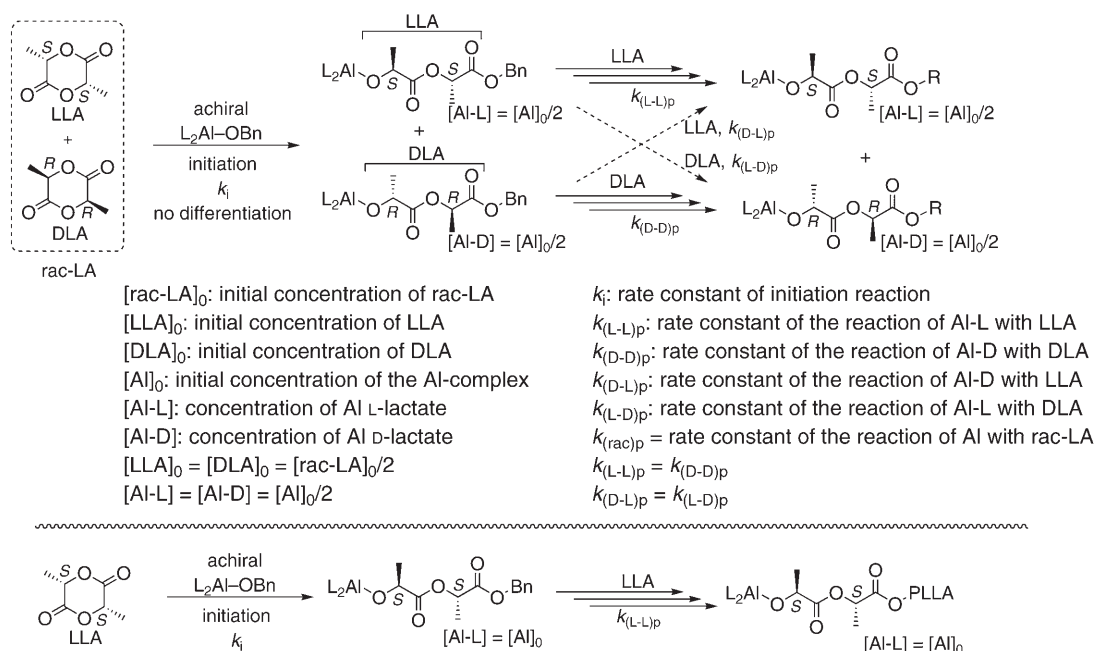
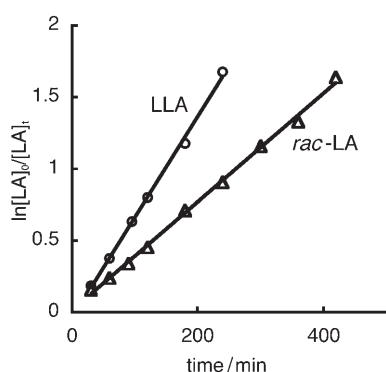
First of all, the reaction order of [*rac*-LA] was examined ($[\text{rac-LA}]_0/[\text{Al}]_0=100$, $[\text{Al}]_0=0.010$ M, $[\text{rac-LA}]_0=1.0$ M). The linearity of time versus $\ln[\text{rac-LA}]_0/[\text{rac-LA}]_t$ plots ($[\text{rac-LA}]_t$ is the concentration of *rac*-LA at time t) indicated that the present ROP is first order in [*rac*-LA] (Eq. (1)), where $k_{(\text{rac})\text{app}}$ is the apparent rate constant of the reaction of *rac*-LA). The slopes ($k_{(\text{rac})\text{app}}$) of the linear plots for four initial concentrations of complex **9** ($[\text{Al}]_0=5.0 \times 10^{-3}$, 10×10^{-3} , 15×10^{-3} , and 20×10^{-3} M) were 1.67×10^{-3} , 3.78×10^{-3} , 5.10×10^{-3} , and $6.67 \times 10^{-3} \text{ min}^{-1}$, respectively. The linear plots of the relationship between $[\text{Al}]_0$ and $k_{(\text{rac})\text{app}}$ also indicated that the ROP is first order in $[\text{Al}]_0$ (Eq. (2)). Accordingly, the kinetic rate equations of *rac*-LA and LLA polymerizations can be expressed as Equations (3) and (4). The $k_{(\text{rac})\text{p}}$ value for the ROP of *rac*-LA with **9** was obtained experimentally ($k_{(\text{rac})\text{p}}=0.378 \text{ min}^{-1} \cdot \text{M}^{-1}$). Similarly, $k_{(\text{L-L})\text{p}}$ was found to be $0.70_0 \text{ min}^{-1} \cdot \text{M}^{-1}$ from the slope of the time vs. $\ln([\text{LA}]_0/[\text{LA}]_t)$ plots for the ROP of LLA (Figure 3).

$$-d[\text{rac-LA}]/dt = k_{(\text{rac})\text{app}}[\text{rac-LA}]_t \quad (1)$$

$$k_{(\text{rac})\text{app}} = k_{(\text{rac})\text{p}}[\text{Al}]_0 \quad (2)$$

$$-d[\text{rac-LA}]/dt = k_{(\text{rac})\text{p}}[\text{Al}]_0[\text{rac-LA}]_t \quad (3)$$

$$-d[\text{LLA}]/dt = k_{(\text{L-L})\text{p}}[\text{Al}]_0[\text{LLA}]_t \quad (4)$$

Scheme 7. Kinetic parameters of the stereoselective ROP of *rac*-LA and LLA via CEM.Figure 3. Kinetic studies using complex **9**. Polymerization conditions: toluene; 70 °C; $[LLA]_0 = [rac-LA]_0 = 1.0 \text{ M}$; $[LA]_0/[Al]_0 = 100$.

In the ROP of *rac*-LA, the initiation reaction occurs without differentiation between the two enantiomers. Once the aluminum complex **9** has incorporated LLA or DLA, the chain-end chirality derived from the monomer strongly differentiates an enantiomer with the same chiral sense from one that has the opposite chiral sense, and the monomer with the same chiral sense preferentially enters the reaction site for the propagation reaction. The rate of polymerization of each enantiomer should be as depicted in Equations (5) and (6). In the living ROP of *rac*-LA using achiral complex **9**, $k_{(L-L)p} = k_{(D-D)p}$, $[Al-L] = [Al-D] = [Al]_0/2$, $[LLA]_t = [DLA]_t$, and $k_{(D-L)p} = k_{(L-D)p}$. Taking into consideration these relationships, the total rate of the ROP of *rac*-LA ([Eq. (5)] + [Eq. (6)]) is given by Equation (7), which can be reduced to Equation (8). Comparing Equation (3) with Equation (8) leads to Equation (9). When ultimate stereoselectivity is achieved, $k_{(D-L)p}$ converges to zero and $k_{(rac)p}$ is $k_{(L-L)p}/2$. The

$k_{(rac)p}$ and $k_{(L-L)p}$ values were obtained from the kinetic experiments of the ROPs of *rac*-LA and LLA, which mean that $k_{(D-L)p}$ can be calculated from Equation (10), which is derived from Equation (9) ($k_{(D-L)p} = 0.054 \text{ min}^{-1} \cdot \text{M}^{-1}$). The stereoselectivity by kinetics (P^k_{meso} , the probability of a *meso*-linkage of the lactide units by kinetics) can be expressed by Equation (11). The P^k_{meso} value is then 0.93 in the ROP of *rac*-LA using complex **9**. This value is slightly lower than that obtained from ^{13}C NMR analysis of poly(*rac*-LA) ($P_{meso} = 0.98$), which may be due to a trace amount of impurities (possibly H_2O) from hygroscopic LLA, whose physical properties are different from those of *rac*-LA (less hygroscopic) in air.

$$-d[LLA]/dt = k_{(L-L)p}[Al-L][LLA]_t + k_{(D-L)p}[Al-D][LLA]_t \quad (5)$$

$$-d[DLA]/dt = k_{(D-D)p}[Al-D][DLA]_t + k_{(L-D)p}[Al-L][DLA]_t \quad (6)$$

$$\begin{aligned}
 -d[rac-LA]/dt &= k_{(L-L)p}([Al]_0/2)([rac-LA]_t/2) \\
 &+ k_{(D-L)p}([Al]_0/2)([rac-LA]_t/2) \\
 &+ k_{(L-L)p}([Al]_0/2)([rac-LA]_t/2) \\
 &+ k_{(D-L)p}([Al]_0/2)([rac-LA]_t/2)
 \end{aligned} \quad (7)$$

$$-d[rac-LA]/dt = 1/2 \times (k_{(L-L)p} + k_{(D-L)p})[Al]_0[rac-LA]_t \quad (8)$$

$$k_{(rac)p} = (k_{(L-L)p} + k_{(D-L)p})/2 \quad (9)$$

$$k_{(D-L)p} = 2k_{(rac)p} - k_{(L-L)p} \quad (10)$$

$$P^k_{meso} = k_{(L-L)p}/(k_{(L-L)p} + k_{(D-L)p}) \quad (11)$$

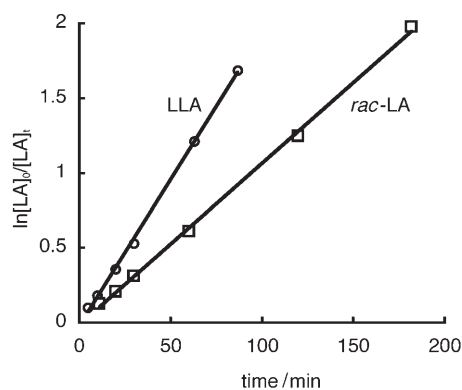


Figure 4. Kinetic studies using complex **8**. Polymerization conditions: toluene; 70 °C; $[LLA]_0 = [rac-LA]_0 = 1.0 \text{ M}$; $[LA]_0/[Al]_0 = 100$.

In contrast to our kinetic studies, which are consistent with the microstructure analysis of poly(*rac*-LA), Chen et al. have concluded that the rates of the ROP of LLA and *rac*-LA with an achiral analogue of complex **8** (Al-*OiPr*) were “approximate” ($k_{(L-L)app} = 7.65 \times 10^{-3} \text{ min}^{-1}$; $k_{(rac)app} = 7.08 \times 10^{-3} \text{ min}^{-1}$).^[39c] Theoretically, this should not be the case. When the kinetics are examined for the same $[Al]_0$, the k_{app} values can be used in Equa-

tion (11) instead of the corresponding k_p values due to Equation (2). The kinetics reported by Chen give $P_{meso}^k = 0.54$, although this is inconsistent with the analysis of the obtained poly(*rac*-LA) ($P_{meso} = 0.89\text{--}0.90$ by Chen and $P_{meso} = 0.9_2$ in entry 1 of Table 3). A P_{meso}^k value of 0.54 means that a *meso* linkage occurs 54% of the time and a *rac* linkage 46% of the time, which should afford an almost random linkage ($P_{meso}^k = 0$ is the limiting value for a heterotactic polymer). Therefore, we decided to re-examine the $k_{(rac)p}$ of complex **8** in the ROP of *rac*-LA and LLA. The $k_{(rac)p}$ and $k_{(L-L)p}$ values were found to be 1.0_8 and $1.9_5 \text{ min}^{-1} \text{ M}^{-1}$, respectively, in our experiments (Figure 4). These kinetic studies produce a stereoselectivity ($P_{meso}^k = 0.90$) that is consistent with the analysis of the poly(*rac*-LA) obtained.

Such an approach can also be used for the ROP of *rac*-LA via an SCM. Feijen has reported the k_{app} values for the systems (*R,R*)-**6**-LLA and (*R,R*)-**6**-DLA ($k_{(L-L)app} = 0.902 \text{ d}^{-1}$, $k_{(L-D)app} = 0.067 \text{ d}^{-1}$).^[60] The P_{iso}^k value calculated from these data ($P_{iso}^k = 0.93$) matches that from the microstructure analysis of the PLA ($P_{iso} = 0.92$).^[61]

Although the kinetic studies require in-depth experiments using well-defined catalysts for living polymerization, we have successfully shown that an option to evaluate the stereoselectivity from the inlet of the reaction system exists.

Stereoselective bulk polymerization of *rac*-LA: Solvent-free bulk polymerization is environmentally benign and unambiguously the most favorable system in industry because of its low cost. We recently reported the stereoselective bulk polymerization of *rac*-LA using **8** prepared in situ,^[62] although the stereoselectivity was only moderate. The bulk polymerization of *rac*-LA (300 equivalents relative to the complex) was therefore examined using isolated complex **9**, for which a higher stereoselectivity was expected than for **8**. The bulk polymerization at 180 °C and reduced pressure ($\approx 1 \text{ Torr}$ at 25 °C) was successful, and the conversion of *rac*-LA reached 91% after 20 min (Table 4, entry 1). LLA polymerized more rapidly, which is consistent with our kinetic studies. As shown in entries 1 and 2 in Table 4, com-

Table 4. Bulk polymerization of LA using complex **9**.^[a]

Entry	LA ^[b]	Temp. ^[c] [°C]	Time [min]	Conv. ^[d] [%]	$M_n^{[e]}$ $\times 10^{-3}$	PDI ^[f]	Yield [%]	$P_{meso}^{[g]}$	$T_m^{[h]}$ [°C]
1	<i>rac</i> -LA	180	20	91	59.9	1.1 ₃	90	0.8 ₄	176
2	LLA	180	10	95	59.3	1.1 ₃	92	–	174
3	<i>rac</i> -LA	130	30	73	43.5	1.0 ₈	69	0.9 ₂	189
4	<i>rac</i> -LA	130	60	97	57.3	1.1 ₀	92	0.9 ₀	188
5	<i>rac</i> -LA	130	120	98	58.9	1.1 ₀	91	0.9 ₁	188

[a] Polymerization conditions: complex **9** (6.7 mg, 0.010 mmol), LA (433 mg, 3.0 mmol); low pressure ($\approx 1 \text{ torr}$) at 25 °C. [b] Lactide. [c] Temperature. [d] The monomer conversion was determined by ¹H NMR spectroscopy. [e] M_n values of the crude samples were estimated by SEC (polystyrene standards, CHCl₃). [f] Polydispersity index (M_w/M_n) of the crude samples by SEC. [g] P_{meso} is the probability of a *meso* linkage between lactide units and was calculated from the ¹³C NMR spectrum of the obtained poly(*rac*-LA). [h] The melting point was measured by DSC. These data were obtained from the second heating.

plex **9** stereoselectively polymerizes *rac*-LA in a living fashion even at 180 °C to afford poly(*rac*-LA) with a T_m value similar to that of homochiral PLLA. At a lower temperature, it takes longer to reach the same high conversion of *rac*-LA, although still occurs in only 30–60 min (Table 4, entries 3 and 4). The polymerization is well-controlled at 130 °C, and the PDI value is virtually unchanged at high conversion and even after a prolonged time (Table 4, entries 4 and 5) due to the bulky substituents of the ligand.

Conclusions

The highly stereoselective ROP of *rac*-LA using *achiral* salen- and homosalen-Al complexes (T_m up to 210 °C, P_{meso} up to 0.9₈) has been described. The following characteristics and advances have been reported in this article: 1) a systematic examination of the substituents has revealed that the steric effects of the ligands at the 3-position of the salicylidene moieties are decisive for the stereoselectivity, and that the structure of the backbone affects the polymerization rate; 2) although complex **9** is chiral in the single crystal, it is achiral in solution due to its flexible conformation; 3) the isotactic polymerization of *rac*-LA proceeds via a CEM with achiral complex **9**; 4) on the basis of the crystal structures of complexes **9** and **11**, a hypothetical mechanism for the ste-

reodifferentiation of LLA and DLA in the propagation step has been proposed that takes into account the steric effects of the substituents, and this is the first experimental approach; 5) it has also been documented that a careful kinetic study can also be undertaken to evaluate the stereoselectivity at the *inlet* of the reaction in addition to the conventional analysis of the poly(*rac*-LA) produced, such as the microstructure (P_{meso}) and the melting temperature (T_m); 6) complex **9** can be used as a catalyst for the stereoselective bulk polymerization, and the living ROP of *rac*-LA is achieved in an environmentally friendly process. The livingness is maintained even at high conversion (98%) at 130°C. It is noteworthy that chiral auxiliaries are not necessary in the metal complex in order to achieve the highly stereoselective ROP of *rac*-LA for isotactic PLA.

Experimental Section

General: All manipulations were carried out using standard Schlenk-line techniques. ^1H NMR spectra were recorded with a Varian Gemini-300 spectrometer in CDCl_3 for calculation of the monomer conversion and with a Bruker Avance 400 for characterization of the complexes and analysis of the polymer microstructure. N_2 was purified using a dry column (T_d (dew point) $\leq -80^\circ\text{C}$; Nikka Seiko) and a gas clean column ($\text{O}_2 \leq 0.002$ ppm; Nikka Seiko). Differential scanning calorimetry (DSC) analyses were performed under N_2 at a heating rate of $10^\circ\text{C}\text{min}^{-1}$ with a Seiko EXSTAR6000. The T_m values were recorded at peak top. The molecular weights of the polymers were estimated by size-exclusion chromatography (SEC) using polystyrene standards (CHCl_3).

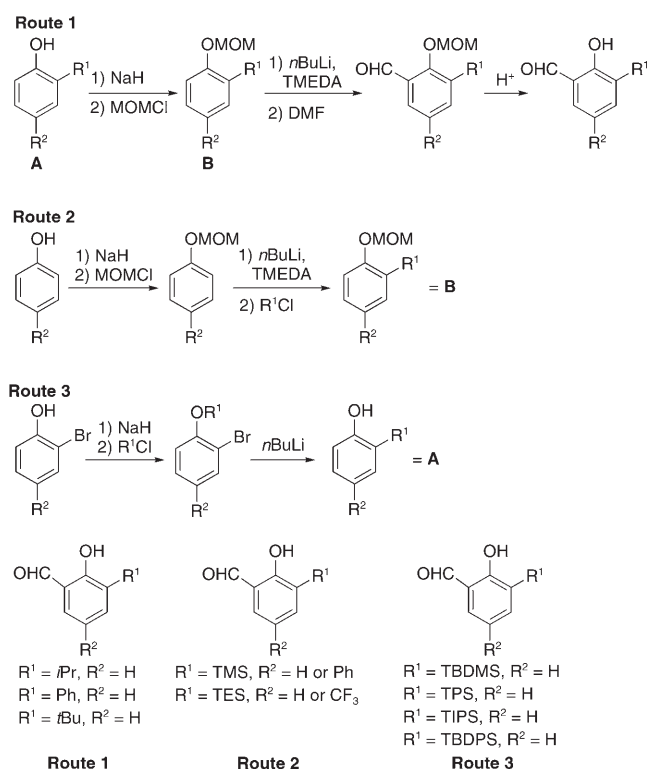
Materials: Toluene (1 L) was first treated with concentrated H_2SO_4 (80 mL) for a few days at room temperature and then washed with H_2O (2×100 mL) and 2N NaOH (100 mL), and again with H_2O (2×100 mL). After drying over Mg_2SO_4 , toluene was heated to reflux in the presence of Na-benzophenone for a few days and distilled prior to use. THF, Et_2O , and C_6D_6 were distilled from Na-benzophenone. BnOH, CH_2Cl_2 , γ -butyrolactone, (*S*)-methyl lactate, and EtOAc were distilled from CaH_2 under N_2 . *rac*-LA and LLA were purchased from Purac and Aldrich and were recrystallized three times from dry EtOAc and stored under N_2 at -40°C . Et_3Al in toluene solution (0.93 M) was purchased from Kanto Chemicals and a 0.10 M Et_3Al solution was prepared by dilution of this solution (1.0 mL, 0.93 mmol) with freshly distilled toluene (8.3 mL); it was stored under N_2 at room temperature. Salicylaldehyde was purchased from Nacalai and 3,5-dibromo-2-hydroxybenzaldehyde was purchased from Aldrich. Other commercially available reagents were used as received.

Ligand synthesis

Salicylaldehyde synthesis: Each aldehyde was prepared according to one of three routes (Scheme 8), except for 3-(3,5-di-*tert*-butylphenyl)-2-hydroxy-5-methylbenzaldehyde and 3-*tert*-butyl-5-chloro-2-hydroxybenzaldehyde. 2-Hydroxy-3,5-dimethylbenzaldehyde, 3,5-di-*tert*-butyl-2-hydroxybenzaldehyde, and 3-bromo-2-hydroxy-5-methylbenzaldehyde were prepared as shown below according to the literature.^[63]

Route 1: synthesis of 2-hydroxy-3-phenylbenzaldehyde: A solution of *o*-phenylphenol (1.0 g, 5.9 mmol) in THF (5 mL) was added to a suspension of 60% NaH in oil (254 mg, 6.4 mmol) in THF (5 mL) at 0°C under N_2 and the resulting mixture was stirred for 1 h. Chloromethyl methyl ether (MOMCl, 0.67 mL, 8.8 mmol) was then added. After stirring the mixture for 4 h at 0°C , the reaction was quenched with saturated aqueous NH_4Cl . The crude product was extracted with Et_2O and dried over Mg_2SO_4 . The corresponding MOM ether (1.2 g, 94%) was obtained after purification by flash column chromatography (hexane/EtOAc = 20/1).

N,N,N',N'-Tetramethylethylenediamine (TMEDA; 1.7 mL, 11 mmol) and *n*BuLi in hexane (1.59 M; 7.0 mL, 11 mmol) were added to the MOM



Scheme 8. Synthesis of the salicylaldehydes.

ether (2.2 g, 10 mmol) in dry Et_2O (10 mL) at 0°C under N_2 and the mixture was stirred for 1 h to afford an orange suspension. This suspension was then cooled to -78°C and DMF (ca. 3 mL) was added. After 5 min, the mixture was placed in a water bath and stirred for an additional hour. The reaction was quenched with saturated aqueous NH_4Cl . The crude product was extracted with Et_2O and dried over Mg_2SO_4 . The corresponding *o*-formylated MOM ether (2.3 g, 91%) was obtained after purification by flash column chromatography (hexane/EtOAc = 15/1).

Concentrated aqueous HCl (ca. 6 mL) was added to the *o*-formylated MOM ether (2.3 g, 9.5 mmol) in THF (15 mL) at room temp. The mixture was stirred for 1 h and then diluted with H_2O . The product was extracted with Et_2O and washed with saturated NaHCO_3 . The ethereal layer was dried over Mg_2SO_4 . 2-Hydroxy-3-phenylbenzaldehyde (1.8 g, 96%) was obtained after purification by flash column chromatography (hexane/EtOAc = 15/1).

2-Hydroxy-3-isopropylbenzaldehyde: The typical procedure was followed starting from 2-isopropylphenol (0.68 mL) to afford the corresponding aldehyde (460 mg) in 55% overall yield.

3-*tert*-Butyl-2-hydroxybenzaldehyde: The typical procedure was followed starting from 2-*tert*-butylphenol (1.6 mL) to afford the corresponding aldehyde (1.2 g) in 71% overall yield.

Route 2: synthesis of 2-hydroxy-3-(trimethylsilyl)benzaldehyde: TMEDA (1.0 mL, 6.6 mmol) and *n*BuLi in hexane (1.59 M; 4.0 mL, 6.4 mmol) were added to a solution of methoxymethyl phenyl ether (720 mg, 5.3 mmol) in dry Et_2O (6 mL) at 0°C under N_2 . The mixture was stirred for 1 h to afford a yellow suspension. TMSCl (0.81 mL, 6.4 mmol) was then added and the mixture was stirred at 0°C for 30 min. After consumption of the starting material (TLC; hexane/EtOAc = 10/1, $R_f = 0.60$ (product)), TMEDA (1.1 mL, 7.3 mmol) and *n*BuLi in hexane (1.59 M; 4.4 mL, 7.0 mmol) were added to the mixture at 0°C under N_2 . The resulting mixture was stirred for 1 h at 0°C and then cooled to -78°C . DMF (1.6 mL, 21 mmol) was added to the mixture. After 15 min, the reaction was quenched with saturated aqueous NH_4Cl . The crude product was extracted with Et_2O and dried over Mg_2SO_4 . The corresponding *o*-formylated MOM ether (1.1 g, 83%) was obtained after purification by flash column

chromatography (hexane/EtOAc=5/1). Deprotection was performed according to route 1.

2-Hydroxy-5-phenyl-3-(trimethylsilyl)benzaldehyde: The typical procedure was followed starting from 4-phenylphenol (1.8 g) to afford the corresponding aldehyde (1.6 g) in 57% overall yield.

2-Hydroxy-3-(triethylsilyl)benzaldehyde: The typical procedure was followed starting from methoxymethyl phenyl ether (770 mg) to afford the corresponding aldehyde (810 mg) in 61% overall yield.

2-Hydroxy-5-(trifluoromethyl)-3-(trimethylsilyl)benzaldehyde: The typical procedure was followed starting from 4-(trifluoromethyl)phenol (1.5 g) to afford the corresponding aldehyde (1.58 g) in 55% overall yield.

Route 3: synthesis of 3-(*tert*-butyldimethylsilyl)-2-hydroxybenzaldehyde: This procedure was similar to one reported in reference [64] with some modifications. *o*-Bromophenol (1.2 mL, 10 mmol) was added to a suspension of 60% NaH in oil (400 mg, 10 mmol) in THF (10 mL) at 0°C under N₂ and the resulting mixture was stirred for 1 h at 0°C. *tert*-Butyldimethylsilyl chloride (TBDMSCl; 1.9 g, 13 mmol) was then added at 0°C. After stirring the mixture for 12 h at room temperature, the reaction was quenched with saturated aqueous NH₄Cl. The crude product was extracted with Et₂O and dried over Mg₂SO₄. The corresponding TBDMS ether (2.7 g, 94%) was obtained after purification by flash column chromatography (hexane).

*n*BuLi in hexane (1.58 M; 5.7 mL, 9.0 mmol) was added to a clear solution of the TBDMS ether (2.5 g, 8.8 mmol) in dry Et₂O (10 mL) at 0°C under N₂. The mixture was stirred for 1 h, then the reaction was quenched with saturated aqueous NH₄Cl. The usual workup gave the pure rearranged compound (1.9 g, quantitative).

Further reactions (protection, formylation (82–87% in 2 steps) and deprotection (96%)) were performed as in route 1 to afford 3-(*tert*-butyldimethylsilyl)-2-hydroxybenzaldehyde (1.55 g, 6.56 mmol).

2-Hydroxy-3-(triphenylsilyl)benzaldehyde: The typical procedure was followed starting from 2-bromophenol (1.2 mL) to afford the corresponding aldehyde (2.2 g) in 58% overall yield.

2-Hydroxy-3-(trisisopropylsilyl)benzaldehyde: The typical procedure was followed starting from 2-bromophenol (1.2 mL) to afford the corresponding aldehyde (2.46 g) in 88% overall yield.

3-(*tert*-Butyldiphenylsilyl)-2-hydroxybenzaldehyde: The typical procedure was followed starting from 2-bromophenol (1.2 mL) to afford the corresponding aldehyde (2.8 g) in 78% overall yield.

Synthesis of 3-(3,5-di-*tert*-butylphenyl)-2-hydroxy-5-methylbenzaldehyde

1-Bromo-3,5-di-*tert*-butylbenzene:^[65] CCl₄ (3.0 mL) was added to a mixture of 1,3,5-tri-*tert*-butylbenzene (1.0 g, 4.1 mmol) and Fe powder (0.245 g, 4.4 mmol) at 0°C under N₂ and Br₂ (0.45 mL, 8.8 mmol) was slowly added to the stirred mixture at 0°C. The resulting mixture was stirred for 33 h at room temperature and was then poured into ice/water. The crude product was extracted with Et₂O, washed with 1 N NaOH and saturated aqueous NaCl, and dried over Mg₂SO₄. 1-Bromo-3,5-di-*tert*-butylbenzene (0.96 g, 88%) was obtained after purification by flash column chromatography (hexane).

3,5-Di-*tert*-butylphenylboronic acid: *n*BuLi in hexane (1.59 M; 1.6 mL, 2.5 mmol) was added to a solution of 1-bromo-3,5-di-*tert*-butylbenzene (583 mg, 2.2 mmol) in dry THF (4 mL) at –78°C under N₂ and the mixture was stirred for 2 h. Trimethylboronic acid (0.73 mL, 6.5 mmol) was added to the resultant suspension at –78°C, and the reaction mixture was gradually warmed to room temperature over 6 h. The reaction was then quenched with 1 N HCl. The crude product was extracted with Et₂O and dried over Mg₂SO₄. 3,5-Di-*tert*-butylboronic acid (407 mg, 80%) was obtained as a mixture of monomer, dimer, and trimer after purification by flash column chromatography (hexane/EtOAc=15/1).

3-(3,5-Di-*tert*-butylphenyl)-2-hydroxy-5-methylbenzaldehyde:^[66] Degassed DME (3.0 mL) and distilled water (1.0 mL) were added to a mixture of 3-bromo-2-hydroxy-5-methylbenzaldehyde (340 mg, 1.6 mmol), 3,5-di-*tert*-butylphenylboronic acid (406 mg, 1.74 mmol), PdCl₂ (32 mg, 0.18 mmol), PPh₃ (208 mg, 0.79 mmol), and K₂CO₃ (333 mg, 2.41 mol) under N₂ and the reaction mixture was heated to reflux at 90°C for 24 h.

After cooling to room temperature, the reaction was quenched with saturated NH₄Cl. The crude product was then extracted with Et₂O and dried over Mg₂SO₄. The product (306 mg, 60%) was obtained upon purification by flash column chromatography (hexane/EtOAc=1/1).

Synthesis of 3-*tert*-butyl-5-chloro-2-hydroxybenzaldehyde: 3-*tert*-Butyl-2-hydroxybenzaldehyde was prepared according to the procedure described in route 1. Chlorination was performed according to a procedure described in literature.^[67] Thus, sulfur chloride (0.58 mL, 7.2 mmol) was slowly added to a mixture of 3-*tert*-butyl-2-hydroxybenzaldehyde (1.0 g, 6.7 mmol) and a catalytic amount of FeCl₃. As soon as chlorination began, the black suspension of the reaction mixture turned red. The reaction mixture was stirred for two days, whereupon the reaction was quenched with saturated Na₂CO₃ and the crude product was extracted with Et₂O, washed with water (3 times), and dried over Mg₂SO₄. The desired product (1.1 g, 5.5 mmol, 75%) was obtained upon purification by flash column chromatography (hexane).

Synthesis of 2-hydroxy-3-(tributylstannyl)benzaldehyde: Methoxymethyl 2-(tributylstannyl)phenyl ether was prepared according to the procedure described in route 2. A solution of *t*BuLi in pentane (1.45 M; 4.0 mL, 5.8 mmol) was added to a solution of methoxymethyl 2-(tributylstannyl)phenyl ether (2.2 g, 5.2 mmol) in Et₂O (5.0 mL) at –78°C under N₂ and the mixture was stirred for 3 h at –78°C to give a pale pink suspension. DMF (1.0 mL, 12.9 mmol) was then added to the mixture. The reaction was quenched with saturated aqueous NH₄Cl and the crude product was extracted with Et₂O and dried over Mg₂SO₄. The corresponding *o*-formylated MOM ether (1.8 g, 3.9 mmol) was obtained after purification by flash column chromatography (hexane/EtOAc=30/1).

NaHSO₄·SiO₂ was prepared according to a procedure described in the literature,^[68] and deprotection was also performed by following a literature procedure.^[69] Dry CH₂Cl₂ (10 mL) and Bu₃Sn-substituted MOM ether (1.56 g, 3.43 mmol) were added to NaHSO₄·SiO₂ (300 mg) under N₂ at room temperature. The mixture was stirred for two days and filtered. The volatiles were removed in vacuo, and the crude product was purified by flash column chromatography (hexane/EtOAc=20/1) to afford the desired product (261 mg, 19%).

Diamine synthesis: 1,2-Diaminoethane, 1,3-diaminopropane, and 1,3-diamino-2,2-dimethylpropane were purchased from TCI and used as received.

Preparation of 2,2-dialkyl-1,3-diaminopropane: See reference [70].

2,2-Dibenzylmalononitrile: A mixture of malononitrile (0.63 mL, 10 mmol), benzyl bromide (2.65 mL, 22 mmol), and tetrabutylammonium bromide (210 mg, 0.65 mmol) was stirred for 30 min at room temperature. Potassium *tert*-butoxide (2.5 g, 22 mmol) was then added slowly at 0°C and the reaction mixture was stirred at room temperature for 16 h. The product was extracted from the reaction mixture with CH₂Cl₂. The crude product was purified by recrystallization from hexane/dichloromethane or hexane/diethyl ether to afford the pure product (821 mg, 33%).

1,3-Diamino-2,2-Dibenzylpropane: A solution of 2,2-dibenzylmalononitrile (571 mg, 2.3 mmol) in dry Et₂O (20 mL) was slowly added to a suspension of LiAlH₄ (224 mg, 5.9 mmol) in dry Et₂O (15 mL) at 0°C. The mixture was heated to reflux for 1 h and then stirred at room temperature for an additional 24 h. Water (1.25 mL) was carefully added to the reaction mixture at 0°C to hydrolyze the unreacted LiAlH₄. The precipitate was filtered off and washed with Et₂O. The ethereal filtrate was treated with concentrated HCl and separated by decantation. After neutralization of the water layer with 2 N aqueous NaOH, the product was extracted with Et₂O (326 mg, 1.28 mmol, 55%).

1,3-Diamino-2,2-diethylpropane: The typical procedure was followed from malononitrile (0.32 mL) to afford the corresponding diamine in 28% overall yield.

Preparation of bis(aminomethyl)dimethylsilane dihydrochloride: See reference [71].

Bis(azidomethyl)dimethylsilane: Bis(chloromethyl)dimethylsilane (1.5 mL, 10.3 mmol) was added to a suspension of sodium azide (2.0 g, 30.8 mmol) in dry DMF (30 mL) and the mixture was heated to 50°C for 26 h. The reaction was then quenched with water (300 mL) and the product was extracted with hexane. After the solution was dried over

Mg₂SO₄, the volatiles were evaporated to afford the product (1.6 g, 9.54 mmol) in 93% yield.

Bis([*N*-(*tert*-butoxycarbonyl)aminomethyl]dimethylsilane): A mixture of bis(azidomethyl)dimethylsilane (919 mg, 5.4 mmol), PtO (98 mg, 0.43 mmol), and (Boc)₂O (2.3 mL, 10.8 mmol) in EtOH (30 mL) was stirred at room temp. for 28 h under H₂. After filtration of the reaction mixture, the crude product was purified by flash column chromatography (hexane/EtOAc=4/1) to afford the desired product (257 mg, 0.81 mmol, 15%).

Bis(aminomethyl)dimethylsilane dihydrochloride: Concentrated aqueous HCl (30 mL) was added to bis([*N*-(*tert*-butoxycarbonyl)aminomethyl]dimethylsilane (257 mg, 0.81 mmol) and the mixture was stirred at room temperature for 1 h. The reaction mixture was then heated to reflux for 12 h and the volatiles were subsequently evaporated to afford the desired product (162 mg, quantitative) as a white solid.

Ligand synthesis: All ligands were prepared by condensation of two equivalents of the corresponding salicylaldehyde with the diamine in EtOH.

General procedure: synthesis of *N,N'*-bis-[3-(*tert*-butyldimethylsilyl)salicylidene]-2,2-dimethyl-1,3-propanediamine: 1,3-Diamino-2,2-dimethylpropane was added to a solution of 3-(*tert*-butyldimethylsilyl)-2-hydroxybenzaldehyde (1.5 g, 6.35 mmol) in EtOH (10 mL) at room temperature and the mixture was stirred for several hours to afford a yellow suspension. After filtration, the product was recrystallized from EtOH/CHCl₃ to give a yellow, crystalline solid (1.67 g, 3.10 mmol, 98% yield). M.p. 113–114°C; ¹H NMR (400 MHz, CDCl₃): δ = 13.58 (s, 2H; OH), 8.33 (s, 2H; ArCHN), 7.43 (dd, *J* = 2.0, 7.2 Hz, 2H; ArH), 7.28 (dd, *J* = 2.0, 7.2 Hz, 2H; ArH), 6.89 (t, *J* = 7.4 Hz, 2H; ArH), 3.48 (s, 4H; CH₂CMe₂CH₂), 1.10 (s, 6H; CH₂C(CH₃)₂CH₂), 0.96 (s, 18H; C(CH₃)₃), 0.36 ppm (s, 12H; *t*Bu(CH₃)₂Si); (400 MHz, C₆D₆): δ = 14.08 (s, 2H; OH), 7.90 (s, 2H; ArCHN), 7.61 (dd, *J* = 1.7, 7.2 Hz, 2H; ArH), 7.15 (dd, *J* = 1.7, 7.5 Hz, 2H; ArH), 6.95 (t, *J* = 7.4 Hz, 2H; ArH), 3.10 (s, 4H; CH₂CMe₂CH₂), 1.23 (s, 18H; C(CH₃)₃), 0.88 (s, 6H; CH₂C(CH₃)₂CH₂), 0.62 ppm (s, 12H; *t*Bu(CH₃)₂Si); ¹³C NMR (100 MHz, CDCl₃): δ = 166.15, 166.09, 139.30, 132.80, 124.93, 117.99, 117.77 (Ar and ArCHN), 68.36 (CH₂CMe₂CH₂), 36.34 (CH₂CMe₂CH₂), 27.12 (C(CH₃)₃), 24.57 (CH₂C(CH₃)₂CH₂), 17.68 (C(CH₃)₃), -4.73 ppm (*t*Bu(CH₃)₂Si); (100 MHz, C₆D₆): δ = 166.56, 166.20, 139.57, 133.02, 125.02, 118.31, 118.16 (Ar and ArCHN), 67.96 (CH₂CMe₂CH₂), 35.67 (CH₂CMe₂CH₂), 27.23 (C(CH₃)₃), 24.07 (CH₂C(CH₃)₂CH₂), 17.77 (C(CH₃)₃), -4.60 ppm (*t*Bu(CH₃)₂Si); elemental analysis calcd (%) for C₃₁H₅₀N₂O₂Si₂: C 69.09, H 9.35, N 5.20; found: C 69.10, H 9.32, N 5.01.

1,3-Diamino-*N,N'*-bis(salicylidene)propane: Yellow, crystalline solid (99% yield). ¹H NMR (300 MHz, CDCl₃): δ = 13.45 (s, 2H; OH), 8.38 (s, 2H; ArCHN), 7.35–7.23 (m, 4H; ArH), 6.98–6.85 (m, 4H; ArH), 3.72 (t, *J* = 6.6 Hz, 4H; CH₂CH₂CH₂), 2.12 ppm (quin, *J* = 6.9 Hz, 2H; CH₂CH₂CH₂); ¹³C NMR (75 MHz, CDCl₃): δ = 165.54, 161.19, 132.33, 131.31, 118.76, 118.71 (Ar and ArCHN), 56.76 (CH₂CH₂CH₂), 31.60 ppm (CH₂CH₂CH₂).

1,3-Diamino-*N,N'*-bis(3,5-dimethylsalicylidene)propane: Yellow powder (89% yield). ¹H NMR (300 MHz, CDCl₃): δ = 13.46 (s, 2H; OH), 8.30 (s, 2H; ArCHN), 7.01 (s, 2H; ArH), 6.88 (s, 2H; ArH), 3.70 (t, *J* = 6.6 Hz, 4H; CH₂CH₂CH₂), 2.26 (s, 6H; CH₃), 2.25 (s, 6H; CH₃), 2.09 ppm (quin, *J* = 6.6 Hz, 2H; CH₂CH₂CH₂); ¹³C NMR (75 MHz, CDCl₃): δ = 165.66, 157.20, 134.31, 128.91, 127.13, 125.65, 117.66 (Ar and ArCHN), 56.71 (CH₂CH₂CH₂), 31.67 (CH₂CH₂CH₂), 20.23, 15.32 ppm (CH₃).

1,3-Diamino-*N,N'*-bis(3-isopropylsalicylidene)propane: Yellow syrup (99% yield). ¹H NMR (300 MHz, CDCl₃): δ = 13.77 (s, 2H; OH), 8.38 (s, 2H; ArCHN), 7.29–7.28 (m, 2H; ArH), 7.12–7.09 (m, 2H; ArH), 6.86 (t, *J* = 7.5 Hz, 2H; ArH), 3.73 (t, *J* = 6.6 Hz, 4H; CH₂CH₂CH₂), 3.41 (sext, *J* = 7.2 Hz, 2H; CH(CH₃)₂), 2.12 (quin, *J* = 6.6 Hz, 2H; CH₂CH₂CH₂), 1.26 ppm (d, *J* = 6.9 Hz, 12H; CH(CH₃)₂); ¹³C NMR (75 MHz, CDCl₃): δ = 165.91, 158.64, 136.36, 128.90, 118.35, 118.12 (Ar and ArCHN), 56.69 (CH₂CH₂CH₂), 31.67 (CH₂CH₂CH₂), 26.32 (CH(CH₃)₂), 22.37 ppm (CH(CH₃)₂).

1,3-Diamino-*N,N'*-bis(3-phenylsalicylidene)propane: Deep yellow, crystalline solid (98% yield). ¹H NMR (300 MHz, CDCl₃): δ = 14.07 (s, 2H;

OH), 8.44 (s, 2H; ArCHN), 7.65–7.24 (m, 14H; ArH), 6.96 (t, *J* = 7.8 Hz, 2H; ArH), 3.74 (t, *J* = 6.6 Hz, 4H; CH₂CH₂CH₂), 2.10 ppm (quin, *J* = 6.3 Hz, 2H; CH₂CH₂CH₂); ¹³C NMR (75 MHz, CDCl₃): δ = 165.79, 158.64, 137.80, 133.32, 130.79, 129.84, 129.36, 128.17, 127.15, 118.86, 118.60 (Ar and ArCHN), 56.48 (CH₂CH₂CH₂), 31.51 ppm (CH₂CH₂CH₂).

1,3-Diamino-*N,N'*-bis(3,5-di-*tert*-butylsalicylidene)propane: Yellow powder (68% yield). ¹H NMR (300 MHz, CDCl₃): δ = 13.8 (s, 2H; OH), 8.39 (s, 2H; ArCHN), 7.39 (d, *J* = 2.4 Hz, 2H; ArH), 7.09 (d, *J* = 2.4 Hz, 2H; ArH), 3.71 (t, *J* = 6.6 Hz, 4H; CH₂CH₂CH₂), 2.12 (quin, *J* = 6.6 Hz, 2H; CH₂CH₂CH₂), 1.46 (s, 18H; C(CH₃)₃), 1.31 ppm (s, 18H; C(CH₃)₃); ¹³C NMR (75 MHz, CDCl₃): δ = 166.57, 158.19, 140.10, 136.73, 126.93, 125.88, 117.87 (Ar and ArCHN), 56.69 (CH₂CH₂CH₂), 34.97, 34.05 (C(CH₃)₃), 31.63 (CH₂CH₂CH₂), 31.43, 29.35 ppm (C(CH₃)₃).

1,3-Diamino-*N,N'*-bis(3-*tert*-butyl-5-chlorosalicylidene)propane: Pale yellow powder (91% yield). ¹H NMR (300 MHz, CDCl₃): δ = 13.99 (s, 2H; OH), 8.32 (s, 2H; ArCHN), 7.26 (d, *J* = 2.1 Hz, 2H; ArH), 7.09 (d, *J* = 2.4 Hz, 2H; ArH), 3.74 (t, *J* = 6.6 Hz, 4H; CH₂CH₂CH₂), 2.16 (quin, *J* = 6.8 Hz, 2H; CH₂CH₂CH₂), 1.42 ppm (s, 18H; C(CH₃)₃); ¹³C NMR (75 MHz, CDCl₃): δ = 165.18, 159.16, 139.80, 129.66, 128.45, 122.60, 119.24 (Ar and ArCHN), 56.80 (CH₂CH₂CH₂), 35.01 (C(CH₃)₃), 31.47 (CH₂CH₂CH₂), 29.03 ppm (C(CH₃)₃).

1,3-Diamino-*N,N'*-bis[3-(trimethylsilyl)salicylidene]propane: Yellow powder (99% yield). ¹H NMR (300 MHz, CDCl₃): δ = 13.55 (s, 2H; OH), 8.37 (s, 2H; ArCHN), 7.42 (dd, *J* = 1.8, 7.2 Hz, 2H; ArH), 7.25 (dd, *J* = 1.8, 7.5 Hz, 2H; ArH), 6.88 (t, *J* = 7.2 Hz, 2H; ArH), 3.71 (t, *J* = 6.6 Hz, 4H; CH₂CH₂CH₂), 2.14 (quin, *J* = 6.6 Hz, 2H; CH₂CH₂CH₂), 0.33 ppm (s, 18H; Si(CH₃)₃); ¹³C NMR (75 MHz, CDCl₃): δ = 165.93, 165.80, 137.80, 132.67, 127.26, 118.36, 117.61 (Ar and ArCHN), 56.92 (CH₂CH₂CH₂), 31.61 (CH₂CH₂CH₂), -1.22 ppm (Si(CH₃)₃).

1,3-Diamino-*N,N'*-bis[5-phenyl-3-(trimethylsilyl)salicylidene]propane: Yellow powder (93% yield). ¹H NMR (300 MHz, CDCl₃): δ = 13.62 (s, 2H; OH), 8.45 (s, 2H; ArCHN), 7.63 (d, *J* = 2.4 Hz, 2H; ArH), 7.55–7.51 (m, 4H; ArH), 7.46 (d, *J* = 2.4 Hz, 2H; ArH), 7.44–7.38 (m, 4H; ArH), 7.34–7.28 (m, 2H; ArH), 3.76 (t, *J* = 6.5 Hz, 4H; CH₂CH₂CH₂), 2.18 (quin, *J* = 6.6 Hz, 2H; CH₂CH₂CH₂), 0.37 ppm (s, 18H; Si(CH₃)₃); ¹³C NMR (75 MHz, CDCl₃): δ = 165.87, 165.55, 140.91, 136.66, 131.57, 131.20, 128.83, 127.91, 126.72, 117.67 (Ar and ArC(Ph)N), 56.96 (CH₂CH₂CH₂), 31.51 (CH₂CH₂CH₂), -1.17 ppm (Si(CH₃)₃).

1,3-Diamino-*N,N'*-bis[3-(3,5-di-*tert*-butylphenyl)-5-methylsalicylidene]propane: Sticky solid (99% yield). ¹H NMR (300 MHz, CDCl₃): δ = 13.66 (s, 2H; OH), 8.38 (s, 2H; ArCHN), 7.46 (d, *J* = 1.8 Hz, 4H; Ar(di-*t*Bu)H), 7.41 (t, *J* = 2.0 Hz, 2H; Ar(di-*t*Bu)H), 7.23 (d, *J* = 2.1 Hz, 4H; ArH), 7.03 (d, *J* = 1.8 Hz, 2H; ArH), 3.71 (t, *J* = 6.3 Hz, 4H; CH₂CH₂CH₂), 2.34 (s, 6H; ArCH₃), 2.09 (quin, *J* = 6.6 Hz, 2H; CH₂CH₂CH₂), 2.38 ppm (s, 36H; C(CH₃)₃); ¹³C NMR (75 MHz, CDCl₃): δ = 165.78, 156.27, 150.21, 136.89, 134.35, 130.67, 130.56, 127.50, 123.82, 121.23, 118.60 (Ar and ArCHN), 56.60 (CH₂CH₂CH₂), 34.85 (CH₂CH₂CH₂, C(CH₃)₃), 31.50 (C(CH₃)₃), 20.34 ppm (ArCH₃).

1,3-Diamino-*N,N'*-bis(3,5-dibromosalicylidene)propane: Yellow powder (66% yield). ¹H NMR (300 MHz, CDCl₃): δ = 14.51 (s, 2H; OH), 8.28 (s, 2H; ArCHN), 7.71 (d, *J* = 7.7 Hz, 2H; ArH), 7.34 (d, *J* = 2.4 Hz, 2H; ArH), 3.78 (t, *J* = 6.6 Hz, 4H; CH₂CH₂CH₂), 2.14 ppm (quin, *J* = 6.5 Hz, 2H; CH₂CH₂CH₂); ¹³C NMR (75 MHz, CDCl₃): δ = 164.10, 158.23, 137.88, 132.78, 119.81, 112.42, 109.62 (Ar and ArCHN), 55.72 (CH₂CH₂CH₂), 31.09 ppm (CH₂CH₂CH₂).

1,3-Diamino-2,2-dimethyl-*N,N'*-bis(salicylidene)propane: Yellow, needle-shaped crystals (99% yield). ¹H NMR (300 MHz, CDCl₃): δ = 13.58 (s, 2H; ArOH), 8.34 (s, 2H; ArCHN), 7.32 (t, *J* = 7.5 Hz, 2H; ArH), 7.28 (d, *J* = 7.8 Hz, 2H; ArH), 6.94 (d, *J* = 8.1 Hz, 2H; ArH), 6.89 (t, *J* = 7.4 Hz, 2H; ArH), 3.49 (s, 4H; CH₂CMe₂CH₂), 1.08 ppm (s, 6H; CH₂C(CH₃)₂CH₂); ¹³C NMR (75 MHz, CDCl₃): δ = 165.82, 161.28, 132.36, 131.40, 118.74, 118.66, 116.98 (Ar and ArCHN), 68.10 (CH₂CMe₂CH₂), 36.17 (CH₂CMe₂CH₂), 24.29 ppm (CH₂C(CH₃)₂).

1,3-Diamino-2,2-dimethyl-*N,N'*-bis(3-phenylsalicylidene)propane: Yellow, crystalline solid (99% yield). M.p. 150–151°C; ¹H NMR (300 MHz, CDCl₃): δ = 14.03 (s, 2H; ArOH), 8.40 (s, 2H; ArCHN), 7.65–7.27, 6.96 (m, 16H; ArH), 3.51 (s, 4H; CH₂CMe₂CH₂), 1.06 ppm (s, 6H; CH₂C-

(CH₃)₂CH₂); ¹³C NMR (75 MHz, CDCl₃): δ = 166.13, 158.65, 137.82, 133.41, 130.93, 129.82, 129.40, 128.23, 127.20, 118.92, 118.62 (*Ar* and *ArCHN*), 68.13 (CH₂CMe₂CH₂), 36.18 (CH₂CMe₂CH₂), 24.33 ppm (CH₂C(CH₃)₂CH₂); elemental analysis calcd (%) for C₃₁H₃₀N₂O₂: C 80.49, H 6.54, N 6.06; found: C 80.49, H 6.59, N 5.92.

1,3-Diamino-*N,N'*-bis(3,5-di-*tert*-butylsalicylidene)-2,2-dimethylpropane: Yellow powder (89% yield). M.p. 194°C; ¹H NMR (400 MHz, CDCl₃): δ = 13.89 (s, 2H; ArOH), 8.39 (s, 2H; ArCHN), 7.41 (d, *J* = 2.4 Hz, 2H; ArH), 7.13 (d, *J* = 2.4 Hz, 2H; ArH), 3.50 (s, 4H; CH₂CMe₂CH₂), 1.49 (s, 18H; ArC(CH₃)₃), 1.33 (s, 18H; ArC(CH₃)₃), 1.12 ppm (s, 6H; CH₂C(CH₃)₂CH₂); ¹³C NMR (100 MHz, CDCl₃): δ = 166.75, 158.19, 139.99, 136.66, 126.89, 125.93, 117.87 (*Ar* and *ArCHN*), 68.28 (CH₂CMe₂CH₂), 36.34 (CH₂CMe₂CH₂), 35.07, 34.13 (C(CH₃)₃), 31.50, 29.44 (C(CH₃)₃), 24.57 ppm (CH₂C(CH₃)₂CH₂); elemental analysis calcd (%) for C₃₅H₅₄N₂O₂: C 78.60, H 10.18, N 5.24; found: C 78.60, H 10.12, N 5.24.

1,3-Diamino-2,2-dimethyl-*N,N'*-bis[3-(trimethylsilyl)salicylidene]propane: Yellow powder (72% yield). M.p. 89–91°C; ¹H NMR (300 MHz, CDCl₃): δ = 13.53 (s, 2H; ArOH), 8.33 (s, 2H; ArCHN), 7.42 (dd, *J* = 1.8, 7.2 Hz, 2H; ArH), 7.26 (m, 2H; ArH), 6.88 (t, *J* = 7.5 Hz, 2H; ArH), 3.49 (s, 4H; CH₂C(CH₃)₂CH₂), 1.09 (s, 6H; CH₂C(CH₃)₂CH₂), 0.34 ppm (s, 18H; ArSi(CH₃)₃); ¹³C NMR (75 MHz, CDCl₃): δ = 166.13, 166.01, 137.80, 132.78, 118.31, 117.64 (*Ar* and *ArCHN*), 68.44 (CH₂CMe₂CH₂), 36.56 (CH₂CMe₂CH₂), 24.46 (CH₂C(CH₃)₂CH₂), -1.20 ppm (Si(CH₃)₃).

1,3-Diamino-2,2-dimethyl-*N,N'*-bis[5-phenyl-3-(trimethylsilyl)salicylidene]propane: Yellow, crystalline solid (92% yield). M.p. 143–144°C; ¹H NMR (300 MHz, CDCl₃): δ = 13.61 (s, 2H; ArOH), 8.43 (s, 2H; ArCHN), 7.64 (d, *J* = 2.4 Hz, 2H; ArH), 7.48 (d, *J* = 2.4 Hz, 2H; ArH), 7.55–7.31 (m, 10H; ArH), 3.53 (s, 4H; CH₂C(CH₃)₂CH₂), 1.13 (s, 6H; CH₂C(CH₃)₂CH₂), 0.38 ppm (s, 18H; Si(CH₃)₃); ¹³C NMR (75 MHz, CDCl₃): δ = 166.21, 165.62, 140.90, 136.66, 131.57, 131.32, 128.82, 127.87, 126.73, 126.67, 117.70 (*Ar* and *ArCHN*), 68.43 (CH₂CMe₂CH₂), 36.29 (CH₂CMe₂CH₂), 24.52 (CH₂C(CH₃)₂CH₂), -1.14 ppm (Si(CH₃)₃).

1,3-Diamino-2,2-dimethyl-*N,N'*-bis[3-(triethylsilyl)salicylidene]propane: Yellow powder (55% yield). M.p. 42–44°C; ¹H NMR (400 MHz, CDCl₃): δ = 13.54 (s, 2H; ArOH), 8.34 (s, 2H; ArCHN), 7.41 (dd, *J* = 1.7, 7.2 Hz, 2H; ArH), 7.28 (dd, *J* = 1.6, 7.2 Hz, 2H; ArH), 6.89 (t, *J* = 7.4 Hz, 2H; ArH), 3.50 (s, 4H; CH₂CMe₂CH₂), 1.11 (s, 6H; CH₂C(CH₃)₂CH₂), 1.02–0.88 ppm (m, 30H; Si(CH₂CH₃)₃); ¹³C NMR (100 MHz, CDCl₃): δ = 166.19, 138.82, 124.44, 118.18, 117.58 (*Ar* and *ArCHN*), 68.45 (CH₂CMe₂CH₂), 36.70 (CH₂CMe₂CH₂), 24.57 (CH₂C(CH₃)₂CH₂), 7.62, 3.29 ppm (Si(CH₂CH₃)₃).

1,3-Diamino-2,2-dimethyl-*N,N'*-bis[3-(triethylsilyl)-5-(trifluoromethyl)salicylidene]propane: Yellow crystalline solid (78% yield). M.p. 105–106°C; ¹H NMR (300 MHz, CDCl₃): δ = 14.09 (s, 2H; OH), 8.39 (s, 2H; ArCHN), 7.59 (2H, m, ArH), 7.53 (2H, m, ArH), 3.52 (4H, s, CH₂CMe₂CH₂), 1.11 (s, 6H; CH₂C(CH₃)₂CH₂), 1.02–0.88 ppm (m, 30H; Si(CH₂CH₃)₃); ¹³C NMR (75 MHz, CDCl₃): δ = 168.78, 165.55, 135.34, 129.87, 126.36, 120.44, 116.82 (*Ar*, *ArCHN* and *ArCF₃*), 68.13 (CH₂CMe₂CH₂), 36.30 (CH₂CMe₂CH₂), 24.39 (CH₂C(CH₃)₂CH₂), 7.37, 2.95 ppm (Si(CH₂CH₃)₃).

1,3-Diamino-2,2-dimethyl-*N,N'*-bis[3-(triisopropylsilyl)salicylidene]propane: Large, yellow crystals (86% yield). M.p. 127–129°C; ¹H NMR (300 MHz, CDCl₃): δ = 13.66 (s, 2H; OH), 8.32 (s, 2H; ArCHN), 7.45 (dd, *J* = 7.5, 1.8 Hz, 2H; ArH), 7.24 (dd, *J* = 7.8, 1.8 Hz, 2H; ArH), 6.88 (t, *J* = 7.4 Hz, 2H; ArH), 3.46 (s, 4H; CH₂CMe₂CH₂), 1.56 (sext, *J* = 7.4 Hz, 6H; Si(CH(CH₃)₂)₃), 1.13 (d, *J* = 7.5 Hz, 36H; Si(CH(CH₃)₂)₃), 1.08 ppm (s, 6H; CH₂C(CH₃)₂CH₂); ¹³C NMR (75 MHz, CDCl₃): δ = 166.59, 166.27, 139.78, 132.60, 122.85, 118.02, 117.79 (*Ar* and *ArCHN*), 68.21 (CH₂CMe₂CH₂), 36.27 (CH₂CMe₂CH₂), 24.49 (CH₂C(CH₃)₂CH₂), 18.89 (Si(CH(CH₃)₂)₃), 11.56 ppm (Si(CH(CH₃)₂)₃).

1,3-Diamino-2,2-dimethyl-*N,N'*-bis[3-(triphenylsilyl)salicylidene]propane: Yellow solid (47% yield). M.p. 138–140°C; ¹H NMR (300 MHz, CDCl₃): δ = 13.80 (s, 2H; OH), 8.38 (s, 2H; ArCHN), 7.66–7.64 (m, 12H; ArH), 7.45–7.35 (m, 18H; ArH), 7.24 (t, *J* = 7.1 Hz, 2H; ArH), 7.23 (t, *J* = 7.2 Hz, 2H; ArH), 6.81 (t, *J* = 7.4 Hz, 2H; ArH), 3.38 (s, 4H; CH₂C(CH₃)₂CH₂), 0.98 ppm (s, 6H; CH₂C(CH₃)₂CH₂); ¹³C NMR (100 MHz, CDCl₃): δ = 166.51, 165.99, 141.46, 136.47, 134.78, 134.03, 129.30, 127.71,

121.60, 118.51, 117.99 (*Ar* and *ArCHN*), 68.04 (CH₂CMe₂CH₂), 36.23 (CH₂CMe₂CH₂), 24.48 ppm (CH₂C(CH₃)₂CH₂).

1,3-Diamino-2,2-dimethyl-*N,N'*-bis[3-(*tert*-butyldiphenylsilyl)salicylidene]propane: Yellow solid (64% yield). M.p. 81–83°C; ¹H NMR (300 MHz, CDCl₃): δ = 14.01 (s, 2H; OH), 8.33 (s, 2H; ArCHN), 7.60–7.57 (m, 6H; ArH), 7.41–7.33 (m, 12H; ArH), 7.23 (dd, *J* = 7.5, 1.8 Hz, 2H; ArH), 7.17 (dd, *J* = 7.5, 1.8 Hz, 2H; ArH), 6.77 (t, *J* = 7.5 Hz, 2H; ArH), 3.45 (s, 4H; CH₂C(CH₃)₂CH₂), 1.26 (s, 18H; C(CH₃)₃), 1.05 ppm (s, 6H; CH₂C(CH₃)₂CH₂); ¹³C NMR (75 MHz, CDCl₃): δ = 166.34, 166.15, 142.14, 136.37, 135.74, 133.54, 128.92, 127.56, 122.63, 118.36, 117.75 (*Ar* and *ArCHN*), 68.01 (CH₂CMe₂CH₂), 36.30 (CH₂CMe₂CH₂), 29.77 (SiC(CH₃)₃), 24.52 (CH₂C(CH₃)₂CH₂), 18.52 ppm (SiC(CH₃)₃).

1,3-Diamino-2,2-dimethyl-*N,N'*-bis[3-(tributylstannyl)salicylidene]propane: Pale yellow, sticky solid (70% yield). ¹H NMR (300 MHz, CDCl₃): δ = 13.38 (s, 2H; OH), 8.30 (s, 2H; ArCHN), 7.40 (dd, *J* = 7.2, 1.2 Hz, 2H; ArH), 7.21 (dd, *J* = 7.2, 1.2 Hz, 2H; ArH), 6.88 (t, *J* = 7.5 Hz, 2H; ArH), 3.47 (s, 4H; CH₂C(CH₃)₂CH₂), 1.67 (m, 12H; Sn(CH₂CH₂CH₂CH₃)₃), 1.34 (sext, *J* = 7.2 Hz, 12H; Sn(CH₂CH₂CH₂CH₃)₃), 1.13–1.11 (m, 12H; Sn(CH₂CH₂CH₂CH₃)₃), 1.08 (s, 6H; CH₂C(CH₃)₂CH₂), 0.88 ppm (t, *J* = 7.2 Hz, 9H; Sn(CH₂CH₂CH₂CH₃)₃).

1,3-Diamino-*N,N'*-bis(3,5-di-*tert*-butylsalicylidene)-2,2-diethylpropane: Yellow, crystalline solid (54% yield). M.p. 185–186°C; ¹H NMR (400 MHz, CDCl₃): δ = 13.85 (s, 2H; OH), 8.40 (s, 2H; ArCHN), 7.40 (d, *J* = 2.4 Hz, 2H; ArH), 7.11 (d, *J* = 2.4 Hz, 2H; ArH), 3.50 (s, 4H; CH₂CEt₂CH₂), 1.50 (q, *J* = 7.6 Hz, 4H; CH₂C(CH₂CH₃)₂CH₂), 1.49 (s, 18H; C(CH₃)₃), 1.32 (s, 18H; C(CH₃)₃), 0.96 ppm (t, *J* = 7.6 Hz, 6H; CH₂C(CH₂CH₃)₂CH₂); ¹³C NMR (100 MHz, CDCl₃): δ = 166.69, 158.14, 139.96, 136.61, 126.82, 125.90, 117.94 (*Ar* and *ArCHN*), 63.66 (CH₂CEt₂CH₂), 41.00 (CH₂CEt₂CH₂), 35.07, 34.12 (C(CH₃)₃), 31.50, 29.44 (C(CH₃)₃), 25.24, 7.33 ppm (CH₂CH₃).

1,3-Diamino-2,2-dibenzyl-*N,N'*-bis(3,5-di-*tert*-butylsalicylidene)propane: Pale yellow powder (35% yield). M.p. 179–180°C; ¹H NMR (300 MHz, CDCl₃): δ = 13.80 (s, 2H; OH), 8.39 (s, 2H; ArCHN), 7.44 (d, *J* = 2.4 Hz, 2H; ArH), 7.30–7.24 (m, 10H; CH₂ArH), 7.12 (d, *J* = 2.4 Hz, 2H; ArH), 3.47 (s, 4H; CH₂CBn₂CH₂), 2.96 (s, 4H; CH₂C(CH₂Ph)₂CH₂), 1.51 (s, 18H; C(CH₃)₃), 1.33 ppm (s, 18H; C(CH₃)₃); ¹³C NMR (75 MHz, CDCl₃): δ = 167.76, 158.19, 140.24, 137.65, 136.80, 131.00, 128.19, 127.16, 126.44, 126.10, 118.01 (*Ar* and *ArCHN*), 62.99 (CH₂CBn₂CH₂), 42.72 (CH₂CBn₂CH₂), 40.64 (CH₂C(CH₂Ph)₂CH₂), 35.06, 34.08 (C(CH₃)₃), 31.44, 29.38 ppm (C(CH₃)₃).

Synthesis of 1,3-diamino-2,2-dimethyl-*N,N'*-bis[5-phenyl-3-(trimethylsilyl)salicylidene]-2-silapropane: Et₃N (0.46 mL, 3.26 mmol) and a solution of 2-hydroxy-5-phenyl-3-(trimethylsilyl)benzaldehyde (440 mg, 1.63 mmol) in EtOH (2.0 mL) were added to a suspension of bis(amino-methyl)dimethylsilane dihydrochloride (162 mg, 0.84 mmol) in EtOH (2.0 mL) in the presence of 4 Å molecular sieves. The mixture was stirred at room temperature for 48 h, and the obtained precipitate was collected by filtration. The filtrate was washed with hexane and dried in vacuo to afford a pale-green solid (162 mg, 0.26 mmol) in 31% yield. M.p. 165–166°C; ¹H NMR (400 MHz, CDCl₃): δ = 13.45 (s, 2H; ArOH), 8.34 (s, 2H; ArCHN), 7.59 (d, *J* = 2.4 Hz, 2H; ArH), 7.54–7.52 (m, 4H; ArH), 7.44–7.40 (m, 6H; ArH), 7.34–7.30 (m, 2H; ArH), 3.48 (s, 2H; CH₂SiMe₂CH₂), 0.38 (s, 18H; Si(CH₃)₃), 0.25 ppm (s, 6H; CH₂Si(CH₃)₂CH₂); ¹³C NMR (100 MHz, CDCl₃): δ = 163.75, 140.91, 135.88, 130.57, 128.73, 126.70, 126.55 (*Ar* and *ArCHN*), 49.87 (CH₂SiMe₂CH₂), -1.05 (ArSi(CH₃)₃), -5.31 ppm (CH₂Si(CH₃)₂CH₂).

Preparation of catalysts: A solution of Et₃Al in toluene (0.10 M; 0.50 mL, 0.050 mmol) was added to a solution of each ligand (0.050 mmol) in toluene (0.50 mL) under N₂ at room temp. The resulting clear solution was stirred under the appropriate conditions. When THF was used as solvent (Table 1, entry 12), the catalyst was dissolved in THF (1.0 mL) after evaporation of the toluene.

Polymerization: A solution or suspension of the catalyst (0.050 M, 1.0 mL, 0.050 mmol) was added through a cannula to a mixture of *rac*-LA (720 mg, 5.0 mmol) and BnOH in toluene (0.10 M, 0.50 mL, 0.050 mmol) under N₂ at room temperature. The catalyst flask was rinsed with toluene (2.0 mL and 1.5 mL) and the washings were also added to the reaction

mixture. The yellow mixture was heated to $(70 \pm 1)^\circ\text{C}$. The polymerization was monitored by ^1H NMR spectroscopy and SEC analysis of a small amount (ca. 5 mg) of the reaction mixture. After the appropriate time the reaction mixture was cooled to room temperature. Poly(*rac*-LA) was obtained by precipitation from the reaction mixture with cold MeOH (ca. 100 mL).

Synthesis of Al complexes

[*N,N'*-Bis(3,5-di-*tert*-butylsalicylidene)-2,2-dimethyl-1,3-propanediaminato]aluminum(III) benzyloxyde (8): A solution of Et_3Al in toluene (0.93 M; 1.0 mL, 0.93 mmol) was added to a yellow solution of the ligand (494 mg, 0.92 mmol) in toluene (1.0 mL) at room temp. under N_2 and stirred at room temp. until ethane was no longer formed. The reaction mixture was then heated to 70°C for 3 h to give a yellow suspension. BnOH (100 μL , 0.97 mmol) was added at room temperature and the mixture was stirred for 2 h. Toluene (1.5 mL) was added, and the mixture became a light yellow solution upon heating to 70°C . Complex **8** precipitated at room temperature after two days (272 mg, 44%). Crystals suitable for X-ray diffraction were obtained from the toluene solution. ^1H NMR (400 MHz, C_6D_6): $\delta = 7.89$ (d, $J = 2.0$ Hz, 2H; ArH), 7.63 (s, 2H; ArCH=N), 7.36–7.16 (m, 5H; ArH), 7.10 (d, $J = 2.0$ Hz, 2H; ArH), 4.86 (brs, 2H; CH_2Ph), 3.35 (d, $J = 12.2$ Hz, 2H; $\text{CH}^a\text{H}^b\text{CMe}_2\text{CH}^a\text{H}^b$), 2.77 (d, $J = 12.1$ Hz, 2H; $\text{CH}^a\text{H}^b\text{CMe}_2\text{CH}^a\text{H}^b$), 1.93 (s, 18H; ArC(CH_3)₃), 1.49 (s, 18H; ArC(CH_3)₃), 0.68 (s, 3H; $\text{CH}_2\text{C}(\text{CH}_3)_2\text{CH}_2$), 0.51 ppm (s, 3H; $\text{CH}_2\text{C}(\text{CH}_3)_2\text{CH}_2$); ^{13}C NMR (100 MHz, C_6D_6): $\delta = 170.31$, 164.10, 141.18, 138.09, 130.56, 128.53, 127.41, 126.96, 119.05 (Ar and ArCH=N), 67.86 ($\text{CH}_2\text{CMe}_2\text{CH}_2$), 65.90 (CH_2Ar), 36.06 (C(CH_3)₃), 35.43 ($\text{CH}_2\text{CMe}_2\text{CH}_2$), 34.15 (C(CH_3)₃), 31.66, 30.18 (C(CH_3)₃), 25.54, 24.99 ppm ($\text{CH}_2\text{C}(\text{CH}_3)_2\text{CH}_2$).

[*N,N'*-Bis(3-(*tert*-butyldimethylsilyl)salicylidene)-2,2-dimethyl-1,3-propanediaminato]aluminum(III) benzyloxyde (9): A solution of Et_3Al in toluene (0.93 M; 0.51 mL, 0.47 mmol) was added to a yellow solution of the ligand (253 mg, 0.47 mmol) in toluene (0.5 mL) at room temperature under N_2 and stirred at room temperature until ethane was no longer formed. The reaction mixture was then heated to 70°C for 12 h to give a yellow solution. BnOH (51 μL , 0.49 mmol) was added at room temperature and the mixture was stirred for 2 h. Complex **9** precipitated at room temperature overnight. After removal of the supernatant by filtration, the precipitate was washed with toluene (2×1.0 mL) and dried in vacuo to afford a yellow solid (246 mg, 78%). Crystals suitable for X-ray diffraction were obtained from toluene solution at 0°C . ^1H NMR (400 MHz, C_6D_6): $\delta = 7.77$ (dd, $J = 7.2$, 1.6 Hz, 2H; ArH), 7.63 (d, $J = 7.6$ Hz, 2H; CH_2ArH), 7.48 (s, 2H; ArCH=N), 7.36 (t, $J = 7.6$ Hz, 2H; CH_2ArH), 7.26–7.21 (m, 1H; CH_2ArH), 7.08 (dd, $J = 7.6$, 1.6 Hz, 2H; ArH), 6.85 (t, $J = 7.4$ Hz, 2H; ArH), 5.30 (s, 2H; CH_2Ar), 3.68 (d, $J = 10.8$ Hz, 2H; $\text{CH}^a\text{H}^b\text{CMe}_2\text{CH}^a\text{H}^b$), 2.55 (d, $J = 12.4$ Hz, 2H; $\text{CH}^a\text{H}^b\text{CMe}_2\text{CH}^a\text{H}^b$), 1.09 (s, 18H; C(CH_3)₃), 0.72 (s, 6H; *t*Bu(CH_3)₂Si), 0.65 (s, 6H; *t*Bu(CH_3)₂Si), 0.64 (s, 3H; $\text{CH}_2\text{C}(\text{CH}_3)_2\text{CH}_2$), 0.42 ppm (s, 3H; $\text{CH}_2\text{C}(\text{CH}_3)_2\text{CH}_2$); ^{13}C NMR (100 MHz, C_6D_6): $\delta = 171.86$ (Ar), 168.70 (ArCH=N), 143.49, 135.07, 129.39, 129.27, 128.53, 127.14, 126.13, 118.98, 116.43 (Ar), 70.49 ($\text{CH}_2\text{CMe}_2\text{CH}_2$), 66.28 (CH_2Ph), 34.98 ($\text{CH}_2\text{CMe}_2\text{CH}_2$), 27.27 (C(CH_3)₃), 25.42, 23.21 ($\text{CH}_2\text{C}(\text{CH}_3)_2\text{CH}_2$), 18.03 (C(CH_3)₃), -3.36, -3.37 ppm (*t*Bu(CH_3)₂Si).

[2,2-Dimethyl-1,*N,N'*-bis(salicylidene)-1,3-propanediaminato]aluminum(III) benzyloxyde (10): A solution of Et_3Al in toluene (0.93 M; 1.0 mL, 0.93 mmol) was added to a yellow solution of the ligand (290 mg, 0.93 mmol) in toluene (1.0 mL) at room temperature under N_2 and stirred at room temperature until ethane was no longer formed. The reaction mixture was then heated to 70°C for 4 h to give a yellow suspension. BnOH (96 μL , 0.93 mmol) was added at room temperature and the mixture was stirred for a few minutes at 70°C . Toluene (5.0 mL) and γ -butyrolactone (1.5 mL) were added to the suspension and heated to 70°C to afford a pale-yellow solution. Complex **10** precipitated at room temperature overnight as a white crystalline solid. The supernatant was removed by filtration and the crystals were dried in vacuo. Due to the low solubility of the dimeric complex obtained, unambiguous ^1H and ^{13}C NMR spectra were not obtained. ^1H NMR (300 MHz, $\text{CDCl}_3/\gamma\text{-BL} = 4/1$ (v/v)): $\delta = 7.40$ –7.36 (m, 1H; ArH), 7.35–7.17 (m, 5H; CH_2ArH), 7.82 (s, 1H; ArCH=N), 7.80 (s, 1H; ArCH=N), 7.16–7.12 (m, 1H; ArH), 7.02 (dd, $J =$

7.4, 1.8 Hz, 1H; ArH), 6.87 (d, $J = 7.5$ Hz, 1H; ArH), 6.77 (d, $J = 8.1$ Hz, 1H; ArH), 6.67 (dd, $J = 7.8$, 1.8 Hz, 1H; ArH), 6.61 (t, $J = 7.4$ Hz, 1H; ArH), 6.47 (t, $J = 7.4$ Hz, 1H; ArH), 4.68 (s, 2H; CH_2Ar), 4.75 (d, $J = 11.1$ Hz, 1H; $\text{CH}^a\text{H}^b\text{CMe}_2\text{CH}^a\text{H}^b$), 3.50 (d, $J = 10.8$ Hz, 1H; $\text{CH}^a\text{H}^b\text{CMe}_2\text{CH}^a\text{H}^b$), 3.12 (d, $J = 11.4$ Hz, 1H; $\text{CH}^a\text{H}^b\text{CMe}_2\text{CH}^a\text{H}^b$), 2.75 (d, $J = 12.0$ Hz, 1H; $\text{CH}^a\text{H}^b\text{CMe}_2\text{CH}^a\text{H}^b$), 1.01 (s, 3H; $\text{CH}_2\text{C}(\text{CH}_3)_2\text{CH}_2$), 0.90 ppm (s, 3H; $\text{CH}_2\text{C}(\text{CH}_3)_2\text{CH}_2$).

[*N,N'*-Bis(3-(*tert*-butyldimethylsilyl)salicylidene)-2,2-dimethyl-1,3-propanediaminato]aluminum(III) (*S*)-methyl lactate (11): A solution of Et_3Al in toluene (0.93 M; 0.50 mL, 0.47 mmol) was added to a yellow solution of the ligand (254 mg, 0.47 mmol) in toluene (0.5 mL) at room temperature under N_2 and stirred at room temperature until ethane was no longer formed. The reaction mixture was then heated to 70°C for 12 h to give a yellow solution. (*S*)-Methyl lactate (50 μL , 0.52 mmol) was added at room temperature, and the mixture was heated to 70°C for 1 h. Complex **11** precipitated upon storage of the solution at 0°C . After removal of the supernatant by filtration, the precipitate was rinsed with toluene (2×1.0 mL) at 0°C and dried in vacuo to afford a yellow, crystalline solid (192 mg, 54%). Crystals suitable for X-ray diffraction were obtained from cold toluene. ^1H NMR (400 MHz, C_6D_6): $\delta = 7.78$ –7.74 (m, 2H; ArH), 7.62 (s, 1H; ArCH=N), 7.54 (s, 1H; ArCH=N), 7.26–7.08 (m, 2H; ArH), 6.852 (t, $J = 7.4$ Hz, 1H; CH_2ArH), 6.850 (t, $J = 7.4$ Hz, 1H; ArH), 4.91 (brs, 1H; OCH(Me)COOMe), 4.45 (brs, 2H; $\text{CH}^a\text{H}^b\text{CMe}_2\text{CH}^a\text{H}^b$), 3.29 (s, 3H; OCH(Me)COOCH₃), 2.63 (d, $J = 11.6$ Hz, 2H; $\text{CH}^a\text{H}^b\text{CMe}_2\text{CH}^a\text{H}^b$), 1.63 (brs, 3H; OCH(CH_3)COOMe), 1.12 (s, 9H; C(CH_3)₃), 1.08 (s, 9H; C(CH_3)₃), 0.55 (s, 12H; *t*Bu(CH_3)₂Si), 0.84 (s, 3H; $\text{CH}_2\text{CCH}_3\text{MeCH}_2$), 0.66 ppm (s, 3H; $\text{CH}_2\text{CMe}(\text{CH}_3)\text{CH}_2$); ^{13}C NMR (100 MHz, C_6D_6): $\delta = 189.19$ (OCH(Me)COOMe), 172.95, 172.53 (Ar), 167.55, 167.16 (ArCH=N), 142.88, 142.62, 135.19, 135.06, 129.04, 128.93, 119.73, 119.65, 115.26, 115.09 (Ar), 71.56 ($\text{CH}_2\text{CMe}_2\text{CH}_2$), 71.22 ($\text{CH}_2\text{CMe}_2\text{CH}_2$), 68.27 (OCH(Me)COOMe), 53.64 (OCH(Me)-COOCH₃), 36.19 ($\text{CH}_2\text{CMe}_2\text{CH}_2$), 27.54 (C(CH_3)₃), 27.43 (C(CH_3)₃), 26.00 ($\text{CH}_2\text{C}(\text{CH}_3)_2\text{CH}_2$), 22.76 ($\text{CH}_2\text{C}(\text{CH}_3)_2\text{CH}_2$), 22.38 (OCH(CH_3)COOMe), 18.06 (C(CH_3)₃), 18.04 (C(CH_3)₃), -3.47 (*t*Bu(CH_3)₂Si), -3.54 (*t*Bu(CH_3)₂Si), -3.73 ppm (*t*Bu(CH_3)₂Si).

Polymerization

Typical procedure: (Table 3, entry 4) A solution of complex **9** in toluene (0.050 M, 0.40 mL, 0.020 mmol) was added to a mixture of *rac*-LA (288 mg, 2.0 mmol) in toluene (1.6 mL) under N_2 at room temperature and the mixture heated to $(70 \pm 1)^\circ\text{C}$. The polymerization was monitored by ^1H NMR spectroscopy and SEC analysis of a small amount (ca. 5 mg) of the reaction mixture. After 14 h, the reaction mixture was cooled to room temp. Poly(*rac*-LA) was obtained by precipitation from the reaction mixture with cold MeOH (ca. 20 mL). The polymerization of entry 3 in Table 3 was conducted as described here, except for addition of BnOH (2.1 μL) to the *rac*-LA.

Bulk polymerization

Typical procedure: (Table 4, entry 2) *rac*-LA (435 mg, 3.0 mmol) and complex **9** (6.7 mg, 0.010 mmol) were placed into a glass bomb in a dry box. Out of the box, the reactor was placed under reduced pressure (≈ 1 Torr) at room temperature, immersed in an oil bath at 180°C , and the mixture stirred for 20 min. The reactor was then rapidly cooled in a water bath and the poly(*rac*-LA) obtained was dissolved in CHCl_3 . A small amount of the crude solution was used to measure the ^1H NMR spectrum (determination of the monomer conversion) and perform an SEC analysis. Poly(*rac*-LA) was purified by precipitation from the solution with cold MeOH.

Acknowledgements

A grant from the Sumitomo Foundation (2002–2003), a Grant-in-Aid for Young Scientists for Scientific Research (2004–2005, no. 16750094), and a Grant-in-Aid for Scientific Research (C) (2006–2008, no. 18550108) from the Ministry of Education, Culture, Sports, Science, and Technology, Japan, are gratefully acknowledged. R.I. is grateful for a JSPS Research Fellowship for Junior Scientists.

- [1] a) J. V. Seppälä, H. Korhonen, J. Kylmä, J. Tuominen in *Biopolymers, Vol. 3b* (Eds.: A. Steinbüchel, Y. Doi), Wiley-Interscience, Weinheim, **2001**, pp. 327–370; b) A. Duda, S. Penczek, in *Biopolymers, Vol. 3b* (Eds.: A. Steinbüchel, Y. Doi), Wiley-Interscience, Weinheim, **2001**, pp. 371–429; c) H. Tsuji in *Biopolymers, Vol. 4* (Eds.: A. Steinbüchel, Y. Doi), Wiley-Interscience, Weinheim, **2001**, pp. 129–178; d) M. Okada, *Prog. Polym. Sci.* **2002**, *27*, 87; e) E. Chiellini, R. Solaro, *Adv. Mater.* **1996**, *8*, 305; f) T. Hayashi, *Prog. Polym. Sci.* **1994**, *19*, 663.
- [2] a) Contamination of 15% of meso-LA, that is, contamination of 7–8% of the D-lactic acid unit, makes the resulting polymer no longer crystallizable: R. E. Drumright, P. R. Gruber, D. E. Henton, *Adv. Mater.* **2000**, *12*, 1841; b) J.-R. Sarasua, R. E. Prud'homme, M. Wisniewski, A. Le Borgne, N. Spassky, *Macromolecules* **1998**, *31*, 3895.
- [3] a) Y. Ikada, K. Jamshidi, H. Tsuji, S. H. Hyon, *Macromolecules* **1987**, *20*, 904; b) H. Tsuji, F. Horii, S. H. Hyon, Y. Ikada, *Macromolecules* **1991**, *24*, 2719.
- [4] T_m of homochiral PLLA: a) 162°C: N. Yui in *Polymeric Materials Encyclopedia, Vol. 10* (Ed.: J. C. Salamone), CRC Press, Boca Raton, **1996**, p. 7947; b) 164°C: PLLA ($M_n=12400$ by SEC) synthesized in our lab using Al(O i Pr) $_3$; c) 174°C: PLLA (see entry 2 in Table 4; $M_n=59300$ by SEC) synthesized in bulk using complex **9**; d) 180°C: A. Södergrård, M. Stolt, *Prog. Polym. Sci.* **2002**, *27*, 1123.
- [5] O. Wachsen, K. H. Reichert, R. P. Kriiger, H. Muchb, G. Schulz, *Polym. Degrad. Stab.* **1997**, *55*, 225.
- [6] N. Yui, P. J. Dijkstra, J. Feijen, *Makromol. Chem.* **1990**, *191*, 481.
- [7] P. Dubois, C. Jacobs, R. Jérôme, P. Teyssié, *Macromolecules* **1991**, *24*, 2266.
- [8] Some heterotacticity of PLA has been reported: K. A. M. Thakur, R. T. Kean, E. S. Hall, J. J. Kolstad, E. J. Munson, *Macromolecules* **1998**, *31*, 1487.
- [9] Reviews: a) Z. Zhong, P. J. Dijkstra, J. Feijen, *J. Biomater. Sci. Polym. Ed.* **2004**, *15*, 929; b) O. Dechy-Cabaret, B. Martin-Vaca, D. Bourissou, *Chem. Rev.* **2004**, *104*, 6147; c) K. Nakano, N. Kosaka, T. Hiyama, K. Nozaki, *Dalton Trans.* **2003**, 4039; d) G. W. Coates, *J. Chem. Soc. Dalton Trans.* **2002**, 467; e) B. J. O'Keefe, M. A. Hillmyer, W. B. Tolman, *J. Chem. Soc. Dalton Trans.* **2001**, 2215. The exciting stereoselective ROP of β -butyrolactone was reported recently: f) A. Amgoune, C. M. Thomas, S. Ilinca, T. Roisnel, J.-F. Carpentier, *Angew. Chem.* **2006**, *118*, 2848; *Angew. Chem. Int. Ed.* **2006**, *45*, 2782.
- [10] The stereoselective ROP of rac-LA in an anionic mechanism with inversion of the chiral carbon (S_N2) may afford syndiotactic PLA, although it has not yet been reported.
- [11] N. Spassky, M. Wisniewski, C. Pluta, A. Le Borgne, *Makromol. Chem. Phys.* **1996**, *197*, 2627.
- [12] a) K. Majerska, A. Duda, *J. Am. Chem. Soc.* **2004**, *126*, 1026. These authors propose that the Al center of complex **2** in the propagation is not hexacoordinate but tetracoordinate due to intramolecular coordination by the oxygen atom from the acyl group of the PLA chain on the basis of 27 Al NMR measurements (see Supporting Information for this reference). b) Chen et al. have reported that the Al center of the active species in the ground state is pentacoordinate in the solid and in CDCl $_3$: Z. Tang, X. Pang, J. Sun, H. Du, X. Chen, X. Wang, X. Jing, *J. Polym. Sci., Part A: Polym. Chem.* **2006**, *44*, 4932. However, it should be noted that toluene is the polymerization solvent in our system and that CHCl $_3$ clearly slows down the polymerization.
- [13] a) A. Le Borgne, V. Vincens, M. Jouglard, N. Spassky, *Makromol. Chem. Macromol. Symp.* **1993**, *73*, 37; b) M. Wisniewski, A. Le Borgne, N. Spassky, *Makromol. Chem. Phys.* **1997**, *198*, 1227.
- [14] P. A. Cameron, D. Jhurry, V. C. Gibson, A. J. P. White, D. J. Williams, S. Williams, *Macromol. Rapid Commun.* **1999**, *20*, 616.
- [15] C. P. Radano, G. L. Baker, M. R. Smith III, *J. Am. Chem. Soc.* **2000**, *122*, 1552.
- [16] T. M. Ovitt, G. W. Coates, *J. Polym. Sci., Part A: Polym. Chem.* **2000**, *38*, 4686.
- [17] T. M. Ovitt, G. W. Coates, *J. Am. Chem. Soc.* **2002**, *124*, 1316.
- [18] a) A. Bhaw-Luximon, D. Jhurry, N. Spassky, *Polym. Bull.* **2000**, *56*, 31; b) D. Jhurry, A. Bhaw-Luximon, N. Spassky, *Macromol. Symp.* **2001**, *175*, 67.
- [19] For our preliminary reports see: a) N. Nomura, R. Ishii, M. Akakura, K. Aoi, *J. Am. Chem. Soc.* **2002**, *124*, 5938; b) R. Ishii, N. Nomura, T. Kondo, *53rd SPSJ Annual Meeting, Polym. Prepr. Jpn.* **2004**, *53*, IID07; c) R. Ishii, N. Nomura, Y. Yamamoto, T. Kondo, *53rd SPSJ Symposium on Macromolecules Polym. Prepr. Jpn.* **2004**, *53*, 2Pb024.
- [20] a) Z. Zhong, P. J. Dijkstra, J. Feijen, *Angew. Chem.* **2002**, *114*, 4692; *Angew. Chem. Int. Ed.* **2002**, *41*, 4510; b) Z. Zhong, P. J. Dijkstra, J. Feijen, *J. Am. Chem. Soc.* **2003**, *125*, 11291.
- [21] P. Hormnirun, E. L. Marshall, V. C. Gibson, A. J. P. White, D. J. Williams, *J. Am. Chem. Soc.* **2004**, *126*, 2688.
- [22] a) T. R. Jensen, L. E. Breyfogle, M. A. Hillmyer, W. B. Tolman, *Chem. Commun.* **2004**, 2504; b) A. P. Dove, H. Li, R. C. Pratt, B. G. G. Lohmeijer, D. A. Culkun, R. M. Waymouth, J. L. Hedrick, *Chem. Commun.* **2006**, 2881.
- [23] a) M. Cheng, A. B. Attygalle, E. B. Lobkovsky, G. W. Coates, *J. Am. Chem. Soc.* **1999**, *121*, 11583; b) B. M. Chamberlain, M. Cheng, D. R. Moore, T. M. Ovitt, E. B. Lobkovsky, G. W. Coates, *J. Am. Chem. Soc.* **2001**, *123*, 3229; c) M. H. Chisholm, J. Gallucci, K. Phomphrai, *Inorg. Chem.* **2002**, *41*, 2785; d) C.-X. Cai, A. Amgoune, C. W. Lehmann, J.-F. Carpentier, *Chem. Commun.* **2004**, 330; e) H. Ma, G. Melillo, L. Oliva, T. P. Spaniol, U. Englert, J. Okuda, *Dalton Trans.* **2005**, 721; f) M. H. Chisholm, J. Gallucci, K. Phomphrai, *Chem. Commun.* **2003**, 48; g) A. Amgoune, C. M. Thomas, T. Roisnel, J.-F. Carpentier, *Chem. Eur. J.* **2006**, *12*, 169.
- [24] a) T. M. Ovitt, G. W. Coates, *J. Am. Chem. Soc.* **1999**, *121*, 4072; b) M. H. Chisholm, N. W. Eilerts, J. C. Huffman, S. S. Iyer, M. Pacold, K. Phomphrai, *J. Am. Chem. Soc.* **2000**, *122*, 11845.
- [25] For a review see: D. A. Atwood, M. J. Harvey, *Chem. Rev.* **2001**, *101*, 37.
- [26] PLA formed from homochiral **2** is a tapered diblock stereocopolymer PDLA-PLLA, while that from rac-**2** is the multiblock stereocopolymer (PLLA-PDLA) $_n$.
- [27] Coates has underlined the importance of steric bulkiness in the ROP of rac-LA using a achiral β -diketiminatozinc system for heterotactic PLA (see ref. [23b]).
- [28] According to Chisholm's recent studies, the effects of the polymer chain-end cannot be ruled out, even in the SCM: M. H. Chisholm, N. J. Patmore, Z. Zhou, *Chem. Commun.* **2005**, 127.
- [29] Baker and Smith have reported that racemic **2** affords a mixture of enantiomerically enriched PLLA and PDLA and that the mass of the polymer molecules is optically inactive (see ref. [15]).
- [30] An in situ approach using Al salicylaldimine complexes in the ROP of CL has been reported: N. Nomura, T. Aoyama, R. Ishii, T. Kondo, *Macromolecules* **2005**, *38*, 5363.
- [31] S. J. Dzugan, V. L. Goedken, *Inorg. Chem.* **1986**, *25*, 2858.
- [32] For a discussion of the microstructure analysis see ref. [16].
- [33] a) J. E. Kasperczyk, *Macromolecules* **1995**, *28*, 3937; b) J. Coudane, C. Ustariz-Peyret, G. Schwach, M. Vert, *J. Polym. Sci., Part A: Polym. Chem.* **1997**, *35*, 1651.
- [34] Spassky has reported a T_m value of 150°C for the PLA produced with **1** in CH $_2$ Cl $_2$ at 70°C: rac-LA/**1**=75, 95 h, 70% conversion, 36% yield, M_n (SEC)=17,300, M_n (1 H NMR)=8,200, $M_w/M_n=1.20$ (see ref. [13b]).
- [35] a) See ref. [19]. b) The group of Atwood and McKee has independently reported the importance of the methylene number in the ROP of propylene oxide: M.-A. Muñoz-Hernandez, M. L. McKee, T. S. Keizer, B. C. Yearwood, D. A. Atwood, *J. Chem. Soc. Dalton Trans.* **2002**, 410.
- [36] Downfield shifts of the ligands were observed in the 1 H NMR spectra: Ar-OH: $\delta=13.45$ (entry 6) and 14.07 ppm (entry 9); ArCH=N: $\delta=8.38$ (entry 6) and 8.44 (entry 9).
- [37] For reviews of immortal polymerization see: a) T. Aida, S. Inoue, *Acc. Chem. Res.* **1996**, *29*, 39; b) S. Inoue, *J. Polym. Sci., Part A: Polym. Chem.* **2000**, *38*, 2861.

- [38] T. Beila, A. Duda, *J. Polym. Sci., Part A: Polym. Chem.* **1996**, *34*, 1807.
- [39] We have systematically modified the backbone of complex **5**: a) R. Ishii, N. Nomura, K. Aoi, *52nd SPSJ Annual Meeting, Polym. Prepr. Jpn.* **2003**, *52*, IIPb008; b) R. Ishii, N. Nomura, T. Kondo, *Polym. J.* **2004**, *36*, 261; c) Recently, Gibson et al. also reported the effects of the backbone in detail: P. Hornmair, E. L. Marshall, V. C. Gibson, R. I. Pugh, A. J. P. White, *Proc. Natl. Acad. Sci. USA* **2006**, *103*, 15343.
- [40] Since our original reports (refs. [19a] and [39]), Chen et al. have reported the same ROP of *rac*-LA with the same dimethyl-substituted complexes: a) Z. Tang, X. Chen, X. Pang, Y. Yang, X. Zhang, X. Jing, *Biomacromolecules* **2004**, *5*, 965; b) Z. Tang, X. Chen, Y. Yang, X. Pang, J. Sun, X. Zhang, X. Jing, *J. Polym. Sci., Part A: Polym. Chem.* **2004**, *42*, 5974.
- [41] The SEC M_n values of PLA using polystyrene standards must be multiplied by a factor of 0.58 to obtain the approximate values: T. Biela, A. Duda, S. Penczek, *Macromol. Symp.* **2002**, *183*, 1 and references therein.
- [42] CCDC-268019 contains the supplementary crystallographic data for this complex. These data can be obtained free of charge from The Cambridge Crystallographic Data Centre via www.ccdc.cam.ac.uk/data_request/cif.
- [43] CCDC-268020 contains the supplementary crystallographic data for this complex. These data can be obtained free of charge from The Cambridge Crystallographic Data Centre via www.ccdc.cam.ac.uk/data_request/cif.
- [44] a) A. W. Addison, N. T. Rao, J. Reedijk, J. van Rijn, G. C. Verschoor, *J. Chem. Soc. Dalton Trans.* **1984**, 1349; b) M.-A. Muñoz-Hernandez, T. S. Keizer, P. Wei, S. Parkin, D. A. Atwood, *Inorg. Chem.* **2001**, *40*, 6782.
- [45] M.-A. Muñoz-Hernandez, T. S. Keizer, S. Parkin, Y. Zhang, D. A. Atwood, *J. Chem. Crystallogr.* **2000**, *30*, 219. The cif file of the complex is available from the Cambridge Crystallographic Data Centre (CCDC 150896) at www.ccdc.cam.ac.uk/data_request/cif.
- [46] CCDC-268018 contains the supplementary crystallographic data for this complex. These data can be obtained free of charge from The Cambridge Crystallographic Data Centre via www.ccdc.cam.ac.uk/data_request/cif.
- [47] Although we thought that BL was rather inert, it has been pointed out by one of our colleagues that it reacts quite readily with nucleophilic reagents, including Al alkoxides, by the ring-opening, although it does not form a high molar mass homopolymer for thermodynamic reasons. We thank this colleague for this information. See: A. Duda, S. Penczek, Ph. Dubois, D. Mecerreyes, R. Jérôme, *Macromol. Chem. Phys.* **1996**, *197*, 1273.
- [48] An Al complex of ϵ -caprolactone has been reported: J. Lewinsky, P. Horeglad, E. Tratkiewicz, W. Grzenda, J. Lipkowski, E. Kolodziejczyk, *Macromol. Rapid Commun.* **2004**, *25*, 1939.
- [49] See the cif file for the three-dimensional structure of dimeric complex **10**. In sharp contrast, the salen complex **1** (R=Me) displays a chiral dimeric structure in the crystal (Δ,Δ - and Λ,Λ -**1**): D. A. Atwood, J. A. Jegier, D. Rutherford, *Bull. Chem. Soc. Jpn.* **1997**, *70*, 2093.
- [50] CCDC-268021 contains the supplementary crystallographic data for this complex. These data can be obtained free of charge from The Cambridge Crystallographic Data Centre via www.ccdc.cam.ac.uk/data_request/cif.
- [51] Feijen has proposed the formation of a hexacoordinate Al compound during the polymerization based on ^1H NMR data (see ref. [20b]).
- [52] Because of this slow reaction, we inadvertently proposed an activated monomer mechanism in our preliminary report (see ref. [19a] and its Supporting Information).
- [53] Ref. [40a]: $M_n(\text{SEC})=25,700$, $P_{\text{meso}}=0.90$, $T_m=193^\circ\text{C}$; $M_n(\text{SEC})=17,800$, $P_{\text{meso}}=0.90$, $T_m=197^\circ\text{C}$; $M_n(\text{SEC})=8,100$, $P_{\text{meso}}=0.88$, $T_m=201^\circ\text{C}$. Since the T_m values are dependent on the M_n values, caution should be exercised with the M_n values when we compare the T_m values.
- [54] Since our report (ref. [39]), Chen et al. have also reported the structure of **8** (Al-O*i*Pr) in the solid state (see ref. [40]).
- [55] The carbonyl carbons of (alkyl lactate)-Al complexes in the ^{13}C NMR spectrum (C=O-Al) are reported to appear between $\delta=181.8$ and 185.3 ppm: B.-T. Ko, F.-C. Wang, Y.-L. Sun, C.-H. Lin, C.-C. Lin, C.-Y. Kuo, *Polyhedron* **1998**, *17*, 4257.
- [56] S. W. Seidel, T. J. Deming, *Macromolecules* **2003**, *36*, 969.
- [57] Recently, Rzepa et al. have reported an informative computational study on the ROP of *rac*-LA for heterotactic PLA: E. L. Marshall, V. C. Gibson, H. S. Rzepa, *J. Am. Chem. Soc.* **2005**, *127*, 6048. According to this paper, a computational study of the isotactic PLA synthesis from *rac*-LA will be reported in due course.
- [58] Another assumption here is that the coordination sites of the hexacoordinate Al complex are the same positions as those of **11** or **11'**.
- [59] All of the evaluations, as far as we know, were made from the T_m value or the microstructure analysis of the obtained poly(*rac*-LA): a) J. Bellener, M. Wisniewski, A. Le Borgne, *Eur. Polym. J.* **2004**, *40*, 523; b) see refs. [11]–[23]; c) see ref. [24a]. Spassky et al. have referred to “the calculated reactivity ratio (rates of homo/cross propagation)” in ref. [13], but their calculation method is not described. It seems that they used the optical purity of the remaining monomer (analysis before the inlet) or the optical purity of the afforded polymer (analysis of the output) in the polymerizations of lactide with various optical purities. Neither calculation is a direct analysis of the polymerization rates.
- [60] See ref. [20b]. A combination of the data for (*R,R*)-**6**-LLA and (*R,R*)-**6**-DLA was selected because we can exclude the polymer exchange process, which complicates the kinetics, in these systems.
- [61] See ref. [20b]. The P_{iso} value was obtained in the (*R,R*)-**6**-*rac*-LA system. Although the polymer exchange process could be excluded, the afforded polymer should be tapered even at about 21% monomer conversion because the equality of the LLA and DLA concentrations cannot be maintained. Therefore, the analysis of PLA at this monomer conversion should have given a slightly lower P_{iso} value than that of the real one.
- [62] The first stereoselective bulk polymerization of *rac*-LA was reported by Feijen using homochiral and racemic complex **6**, which was slow (see ref. [20]). We have since succeeded by using achiral complex **8**; see ref. [39].
- [63] J. F. Larrow, E. N. Jacobsen, *J. Org. Chem.* **1994**, *59*, 1939.
- [64] K. J. O'Connor, S.-J. Wey, C. J. Burrows, *Tetrahedron Lett.* **1992**, *33*, 1001.
- [65] C. M. D. Komen, F. Bickelhaupt, *Synth. Commun.* **1996**, *26*, 1693.
- [66] M. A. Zhuravel, S. T. Nguyen, *Tetrahedron Lett.* **2001**, *42*, 7925.
- [67] W. D. Watson, *J. Org. Chem.* **1985**, *50*, 2145.
- [68] G. W. Breton, *J. Org. Chem.* **1997**, *62*, 8952.
- [69] C. Ramesh, N. Ravindranath, B. Das, *J. Org. Chem.* **2003**, *68*, 7101.
- [70] F. Qian, J. E. McCusker, Y. Zhang, A. D. Main, M. Chlebowski, M. Kokka, L. McElwee-White, *J. Org. Chem.* **2002**, *67*, 4086.
- [71] V. Van Dorselaer, D. Schirlin, P. Marchal, F. Weber, C. Danzin, *Bioorg. Chem.* **1996**, *25*, 178.

Received: September 11, 2006
Published online: March 6, 2007